INTERNATIONAL SCIENTIFIC JOURNAL

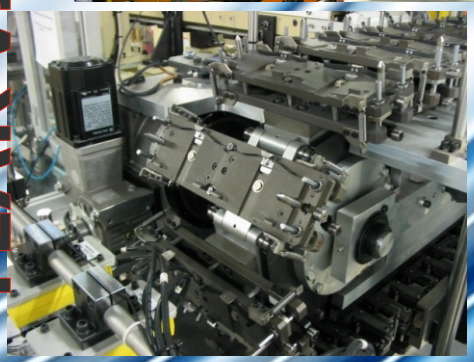
trans & MOTAUTO WORLD

ISSN PRINT 2367-8399
ISSN WEB 2534-8493

YEAR VII, ISSUE 1/2022









SCIENTIFIC TECHNICAL UNION OF MECHANICAL INGENEERING "INDUSTRY 4.0"
108 RAKOVSKI STR., SOFIA 1000, BULGARIA

INTERNATIONAL SCIENTIFIC JOURNAL

TRANS MOTAUTO WORLD

PUBLISHER:

SCIENTIFIC TECHNICAL UNION OF MECHANICAL ENGINEERING INDUSTRY-4.0

108, Rakovski Str., 1000 Sofia, Bulgaria
tel. (+359 2) 987 72 90,
tel./fax (+359 2) 986 22 40**,**
office@stumejournals.com
www.stumejournals.com

ISSN PRINT 2367-8399
ISSN WEB 2534-8493
YEAR VI, ISSUE 1 / 2022

EDITORIAL BOARD

CHIEF EDITOR
Prof. Petar Kolev, Bulgaria

MEMBERS:

Prof. Ahmet H. Ertas, TR	Prof. Massimo Borghi, IT
Prof. Aleksandar Kostikj, MK	Prof. Miho Mihow, BG
Prof. Andrey Ferenets, RU	Prof. Murat Dogruel, TR
Prof. Angel Dimitrov, BG	Prof. Natalia Sidenko, LV
Prof. Beti Angelevska, MK	Prof. Natasa Tomic-Petrovic, RS
Prof. Dainis Berjoza, LV	Prof. Nikolay Georgiev, BG
Prof. Dan Scarpete, RO	Prof. Nikolay Ovchenkov, RU
Prof. Daniela Todorova, BG	Prof. Oleg Sharkov, RU
Prof. Emilia Andreeva-Moschen, AT	Prof. Pepo Yordanov, BG
Prof. Hristo Stanchev, BG	Prof. Polatbeg Zhunisbekov, KZ
Prof. Igor Penkov, EE	Prof. Rinat Kurmaev, RU
Prof. Igor Smirnov, UA	Prof. Rosen Ivanov, BG
Prof. Igor Taratorkin, RU	Prof. Sanjin Troha, HR
Prof. Iliyan Lilov, BG	Prof. Teymuraz Kochadze, GE
Prof. Lech Sitnik, PL	Prof. Tomaz Morchadze, GE
Prof. Ljudmila Boyko, UA	Prof. Vadim Zhmud, RU
Prof. Madaminjon Aripdzanov, UZ	Prof. Valyo Nikolov, BG
Prof. Martin Kendra, SK	Prof. Zoran Jovanovic, RS

RESPONSIBLE SECRETARY:
Prof. Nikolay Tonchev, Bulgaria

C O N T E N T S

TRANSPORT TECHNICS. INVESTIGATION OF ELEMENTS. RELIABILITY

Simulation of the hobbing process of enveloping wormwheels for the calculation of contact pattern and contact lines
Christian Kirchhoff, Linda Becker, Peter Tenberge 3

The vehicle that can move on an accidental field
Cârjali Erol 7

Determination of the quality of welds produced by robotic welding
Janette Brezinová, Ján Hašuľ, Jakub Brezina 11

Research on loading-transport machine parts in order to determine the causes of defects
Rositsa Gavrilova, Boyan Yordanov, Dimitar Krastev, Iliyan Mitov 15

TRANSPORT. SAFETY AND ECOLOGY. LOGISTICS AND MANAGEMENT

Influencing factors on the speed of vehicles in the school and kindergarten zones on the territory of Novi Sad
Milja Simeunović, Zoran Papić, Nenad Saulić 19

Use of innovative methods in the management of tourist transport infrastructure
Gvantsa Arjevanidze, Nargiza Karkashadze, Tinatin Gugeshashvili, Izolda Dangadze 22

Decade of road markings and traffic signs quality testing in Croatia
Dario Babić, Mario Fiolić, Goran Zovak 25

The impact of COV - 19 pandemic on use of public transport in selected city in Slovakia
Daniela Šusteková, Lýdia Kontrová 30

VEHICLE ENGINES. APPLICATION OF FUELS TYPES. EFFICIENCY

Development of an 1D simulation model to optimize performance and emissions of large gas engines
Dimitar Dimitrov, Gernot Kammel, Erich Egert, Nicole Wermuth, Andreas Wimmer 35

Methane number influence on the dual fuel four stroke marine engine performance at high load range
Delyan Hristov 39

Simulation of the hobbing process of enveloping wormwheels for the calculation of contact pattern and contact lines

Christian Kirchhoff[1], Linda Becker[1], Peter Tenberge[1]
Ruhr-University Bochum, Germany[1]
E-mail: Christian.Kirchhoff@rub.de, Linda.Becker@rub.de, Peter.Tenberge@rub.de

Abstract: *The contact pattern and contact line calculation is an essential part of the design of worm gears. The existing calculation algorithms are based on the law of gearing. For this reason, cases like meshing interferences can only be analysed to a limited extent. The simulation of the hobbing process of enveloping wormwheels, introduced here, makes it possible to generate any wheel flank precisely. For the contact pattern calculation, one wheel flank is generated from the cutter geometry and one from the worm geometry. These two generated flanks are brought into contact. For each flank coordinate, the distance to the opposite flank is obtained. The graphical application of this distance over the wheel coordinates results in a contour diagram that is known as the contact pattern. The contact line calculation of worm gears also shows on which part of the flanks power is transmitted at a certain rotational position. For this calculation, the wheel flank generated from the cutter is brought into contact with the worm flank at any angular positions.*
Keywords*: WORM GEARS, ENVELOPING WHEEL, HOBBING PROCESS, CONTACT PATTERN, CONTACT LINES*

1. Introduction

Worm gear units allow high gear ratios in one gear stage and therefore require less mounting space than other gear units that deliver the same gear ratio. Compared to spur gears, they are less efficient due to the high sliding movements, but there are applications in which this is actually an advantage. A good example are worm gear units for elevators. Here, the worm gearing can be designed to be self-locking. This helpfully causes the elevator to move only by the drive of the motor on the worm side and not by the output torque resulting from the weight of the passengers. An additional brake can be avoided in this case. Another positive feature of worm gear units is the high possible overlap of the teeth, which results in very smooth running.

The line contact between the worm and the enveloping wheel requires them to be matched very precisely with each other. The wheel is usually made of centrifugal casting bronze. This shows a good run-in behavior. It means that production-related gear deviations or drive-related deformations with initially high wear can be compensated. During the run-in phase, the wheel flank adapts to the worm geometry and the efficiency improves.

The run-in behavior can be optimized by varying the gear and manufacturing parameters. Small deviations between the worm and cutter geometry prove to be effective. Theoretically congruent flank geometries cannot be paired congruently in real terms, resulting in large wear.

To check the mounting situation of the two gears, a contact pattern test is applied by brushing the wheel flanks and then spinning the gears under load. The basic idea is that the contact pattern should not extend over the entire wheel flank in order to avoid root and edge supports as a result of deformation. However, when noise behavior is a high requirement, the contact pattern is positioned over a relatively large area and towards the root of the tooth (Fig. 1, left). The contact pattern for worm gears exposed to impact and high loads is smaller and positioned toward the tooth tip (Fig. 1, right). [1]

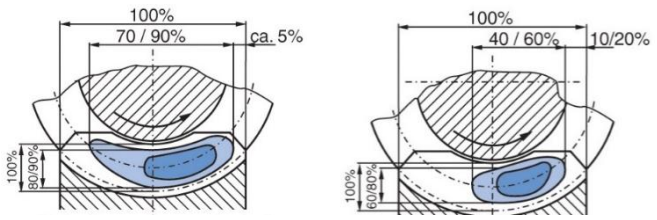


Fig. 1 *Ideal contact patterns for low-noise (left) and highly stressed gearings (right) [1]*

For gearings that are operated in both directions of rotation, the contact pattern is oriented centrally on the gear flank. If the gear unit is used primarily for one direction of rotation, the contact pattern is shifted to the run-out side. This favors the lubricant film buildup and increases the efficiency. In Figure 1, the inlet side is on the left and the outlet side on the right for both gears. [1]

2. Prerequisites and means for solving the problem

The previous section shows that the load profile calculation is an essential part of the design and manufacture of worm gears. In order to save costs and time in the production of a good contact pattern for a specific application, there still exists different software tools that calculates the contact pattern in advance with defined flanks and tool geometry. These programs are based on the law of gearing. The enveloping gear flank contour is determined analytically by the tooth contact to the worm flank. This purely analytical approach leads to problems in critical cases like meshing interferences. Likewise, the calculation of special gears such as worms with a large number of teeth or worms with a very small center pitch angle is not possible.

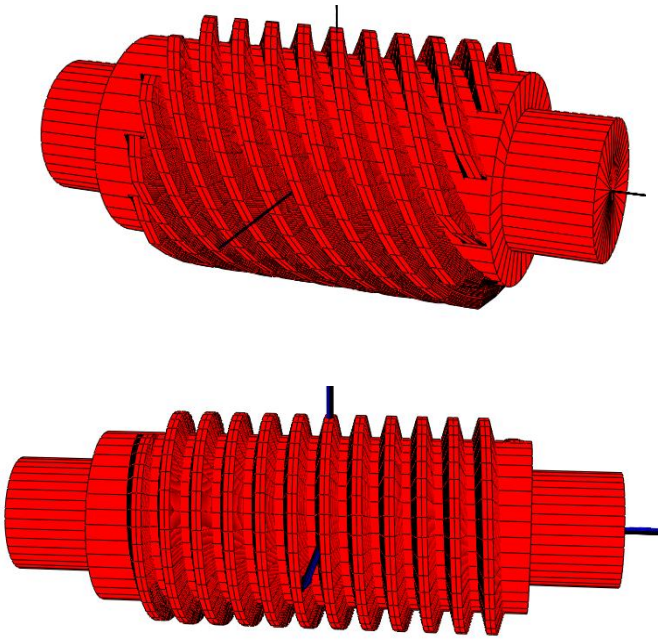


Fig. 2 *Worm with a high number of teeth (left) and with one tooth and a small pitch angle (right)*

3. Solution of the examined problem

To calculate the contact pattern and contact line of any worm gear, a numerical approach is chosen which is presented in the following. The hobbing process of the enveloping gear flank from the tool contour is simulated. This simulation uses a modification of the algorithm already successfully used for spur gears [2]. A surface element is being specified on the wheel blank, which includes the surface within the pitch angle of the wheel. This surface element is defined with two grid boundary functions. One function is located at the tooth tip (Fig.3, black) and one at the tooth root (Fig. 3, green). A certain number of points (Fig.3: 30 points) is defined on both functions. The connections between the respective opposite points of the grid boundaries are made of straight lines (Fig.3, gray), which pass through the volume element as a grid.

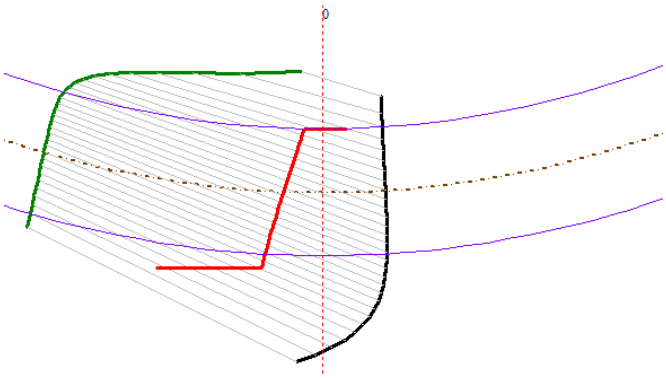


Fig. 3 *Cutter contour and surface element on the wheel blank at pitch position 0°*

This grid is rotated around the wheel axis depending on the position of the cutter geometry, so that the kinematics between the wheel blank and the tool of the hobbing process are correctly reflected. For each grid line, it can be determined in a specific rotational position if and where there is an intersection with the cutter contour. The grid is rotated from the central rotational position (Fig. 3) first to the right and then to the left until no new intersection points are found between the cutter contour and the grid lines that are closer to the tooth root boundary function (green).

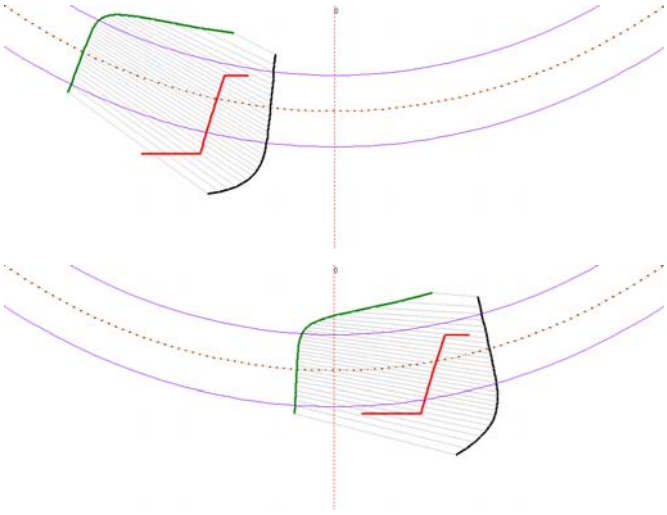


Fig. 4 *Cutter contour and surface element on the wheel blank at -9° (top) and pitch position 11° (bottom)*

During rotation in one direction, the intersection point of each grid line that is closest to the tooth root boundary function is saved from all rotation positions. The connection of all these saved points per grid line, provides the hobbed wheel contour. Any material of the wheel blank that is below these intersection points is removed in the hobbing process. [2]

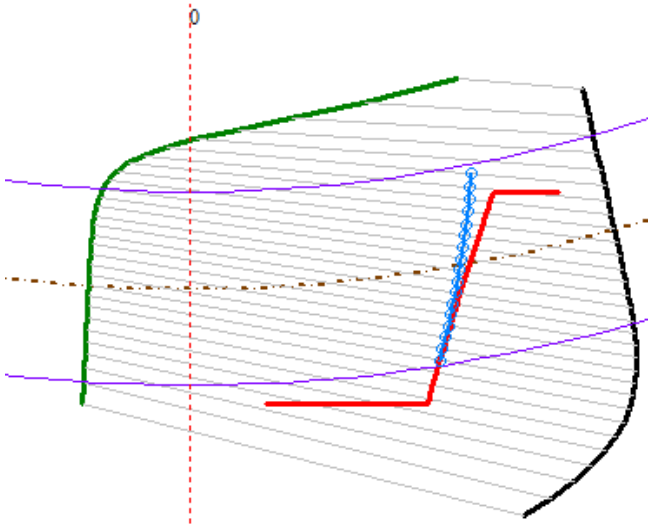


Fig. 5 *Wheel contour (blue) resulting from the hobbing simulation between tooth root and tooth tip (purple) as a sequence of intersection points with minimum distance to the tooth root boundary (green) for each grid line*

In the case of spur gears, it is only necessary to carry out the simulation of the hobbing process in a spur plane of the gear, since the gear contour, apart from the torsion due to the helix angle, does not change over the width of the gear or hardly changes with a clearly defined width crowning. The enveloped wheel contour of a worm gear, on the other hand, has a significant change in shape over the wheel width. For this reason, the hobbing simulation is performed in several parallel sections. In each of these cuts, the 2D cutter contour is required. For this purpose, the contour in the axial section plane of the tool is first determined from the gear data. Predki [3] provides the calculation of the axial section contour for the common flank shape ZA, ZI, ZN, ZC and ZK of worm gears. In addition, the vertical crowning can be included in the form of a parabola according to DIN 3975-1 [4]. By screwing the axial profile geometry around the tool axis, not only the 3D geometry can be derived, but also the 2D contour in the selected parallel sections can be determined.

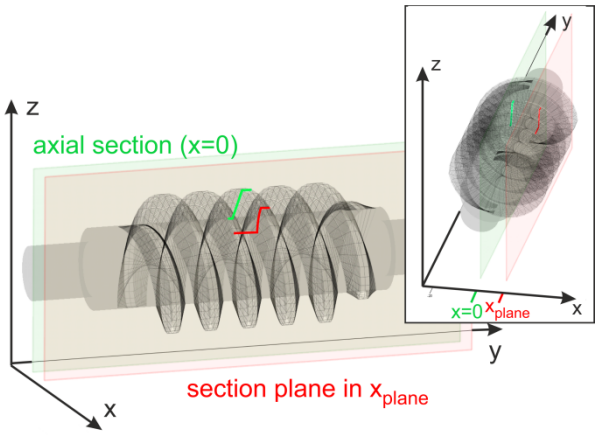


Fig. 6 *3D cutter geometry, axial section profile (green) in axial section plane and calculated tool contour (red) in any section plane.*

Figure 7 shows the calculation algorithm for determining the tool contour in a parallel section plane (yellow) from the axial section plane (x = 0). The contour profile is shown as a red sequence of points. It is possible to determine the coordinates of each point in the plane via an associated screw angle delta. This angle is calculated trigonometrically from the x-coordinate x_{plane} of the plane and the Z-coordinate of the axial section point:

$$\delta = \arcsin\left(\frac{x_{plane}}{z_{plane}}\right) \qquad (1)$$

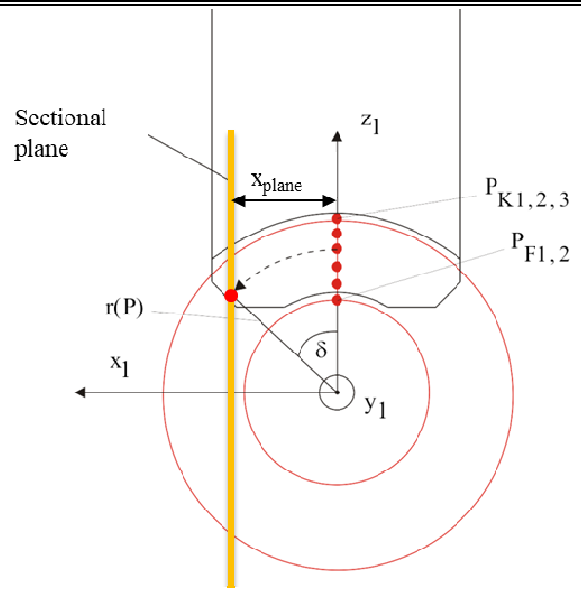


Fig. 7 *Illustration of the determination of the screw angle for determining the tooth contour in a parallel section plane ($x = x_{plane}$) from the axial section plane ($x = 0$)*

In each parallel section, the cutter contour can be calculated in each pitch. With this tool contour, the wheel contour is determined in all parallel section as shown in Figure 5. The separate 2D wheel contours (Fig.8, blue) are combined to form the entire 3D wheel flank. For this purpose, a cubic interpolation is used to generate more grid points over the entire wheel geometry (Fig.8, gray). On the one hand, the number of sections is increased, but also the number of flank points in each of these sections is increased and set to a fixed number. This way, these cuts can be connected and the entire wheel flank is created from the hobbing simulations of each parallel section in detail.

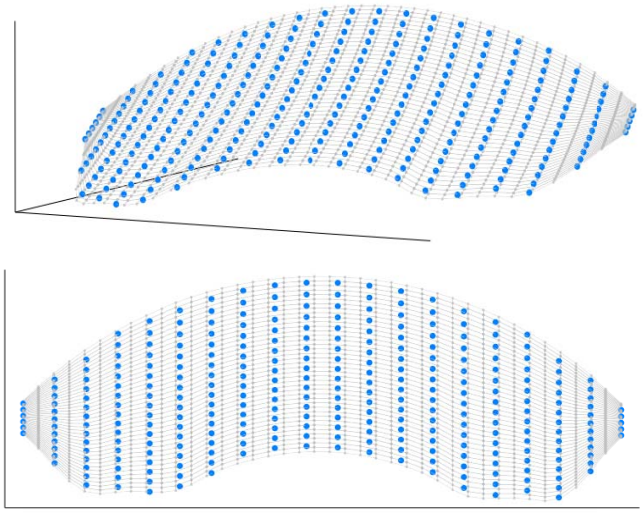


Fig. 8 *Perspective view and radial section of the enveloping wheel contour. The intersection points from the hobbing simulations are gray and the interpolated grid points are blue.*

For illustration purposes, a smaller number of grid lines and section planes as well as interpolation points have been chosen in the figures. To achieve good calculation results, at least 100 grid lines and 30 parallel intersections are selected. The following interpolation is done with at least 40 interpolation sections and 100 points per flank.

For the calculation of the contact pattern, a wheel flank is generated once from the cutter and once from the worm. The wheel flank from the cutter geometry is the real flank before the run-in phase of the worm gear, and the wheel flank from the worm geometry represents the ideal wheel flank after run-in wear. These wheel flanks are rotated towards each other so that they touch at one point.

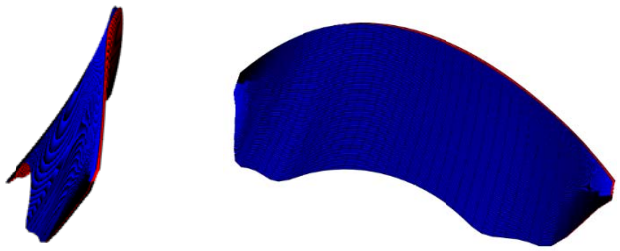


Fig. 9 *Pairing of the two generated enveloping wheel flanks.*

Between all flank points, the distance can be calculated as shown in Figure 10.

$$\text{distance} = \text{radius} \bullet (\alpha_S - \alpha_F) \qquad (2)$$

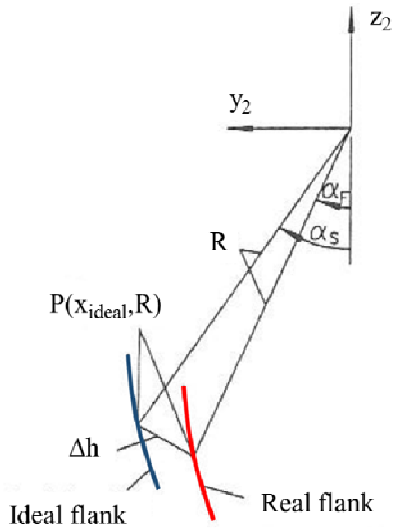


Fig. 10 *Distance calculation between the two wheel flanks*

A contour line diagram is then generated (Fig. 11), on which the flank distance is plotted for each wheel flank coordinate. This contour line diagram is the contact pattern of the gears. It clearly shows where the initial contact zone and consequently the run-in wear will take place. The contact pattern can therefore be used to evaluate how suitable the selected cutter geometry is for generating the wheel flank.

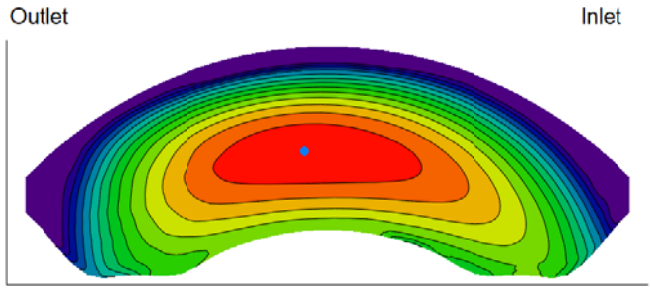


Fig. 11 *Contact pattern – contour line diagram, distance 0 in blue point*

In contrast to the contact pattern, the contact lines are calculated from the flanks actually in contact, which are the wheel flank and the worm flank. The position of the worm flank can be determined from the kinematics of the two gear partners for a given pitch position of the wheel flank. A contact line is automatically set.

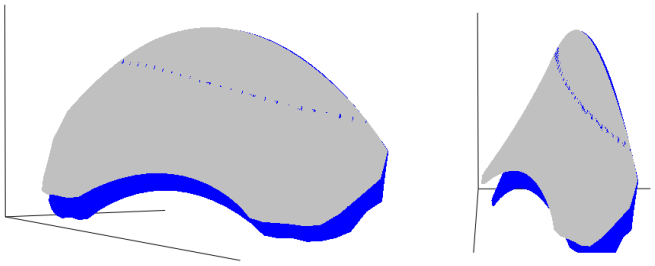


Fig. 12 *Contact line of wheel and worm flank at a specific pitch angle*

In each of the parallel sections of the gear, the point of minimum distance between the flanks is determined. If this point is below a defined limit value, this point counts as a contact point and is part of the contact line. All parallel sections are processed and all found contact points are connected to the contact line. By passing through different pitch positions from the beginning to the end of the tooth contact, the contact line diagrams in the radial section of the worm wheel and in the worm transverse section are obtained.

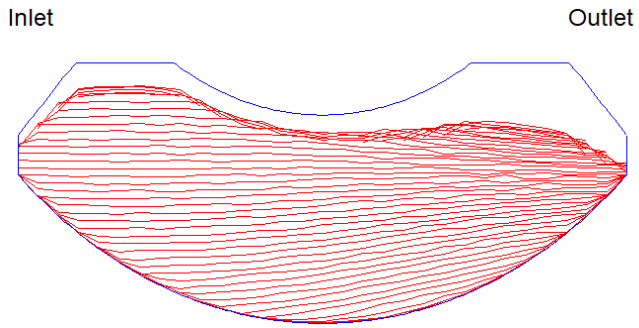


Fig. 13 *Contact lines in the transverse section of the worm*

In addition, the contact lines can be viewed in the top view of the worm. The points that leads to the contact line can also be combined as a meshing line for each parallel section. This allows the length of the contact to be identified.

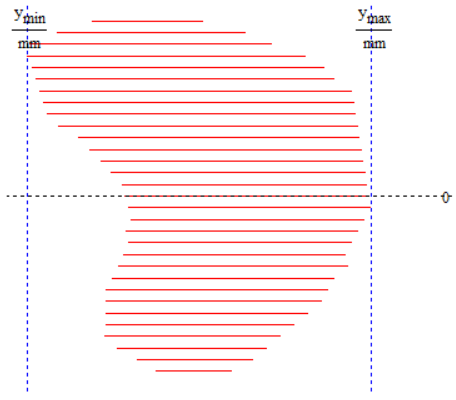


Fig. 14 *Contact lines in the worm face section*

The overlap ε_γ can be determined from minimum (y_{min} = A) and maximum (y_{max} = E) of these mesh lines, which directly indicates the quality of the gearing:

$$\varepsilon_\gamma = \frac{AE}{p_{x1}} = \frac{y_{max} - y_{min}}{p_{x1}} \qquad (3)$$

4. Results and discussion

The developed algorithms were implemented in the software "Trabi 10" at the chair of industrial and automotive drivetrains at Ruhr-University Bochum. This software not only provides the same results for standard gears that can be calculated with existing software, but now also provides results for the mentioned borderline cases (meshing interferences, high number of teeth, etc.). The software is already used in industry and shows a very good fit between theory and practice as can be seen in figure 15.

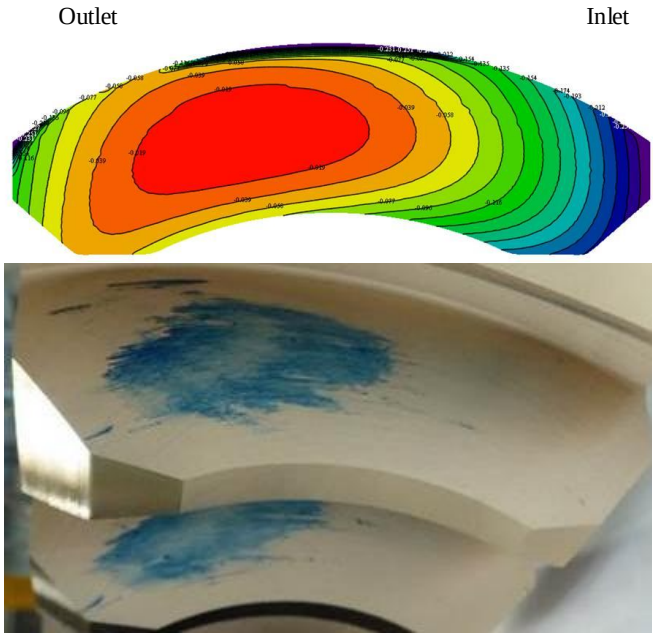


Fig. 15 *Comparison between calculated contact pattern with Trabi 10 (top) and the manufactured contact pattern at "Zahnradfertigung Ott" (bottom)*

5. Conclusion

The software "Trabi 10" with the presented calculation algorithms provides for the first time the possibility to calculate the contact patterns and contact lines of any worm gears without restrictions. Overall, the software is characterized by the fast calculation of many gear variants and the stability of the numerical algorithms. The influence of the various gears and manufacturing parameters on the contact pattern and the contact lines quickly becomes evident and a deep understanding for the correct design of the manufacturing tool is created.

6. References

1. B. Schlecht, *Maschinenelemente 2 Getriebe-Verzahnungen Lagerungen*, Pearson Studium, München (2010)
2. R. Uelpenich, P. Tenberge, *Fast tooth root load capacity optimization based on improved design of hob geometry*, Power Transmissions (2019)
3. W. Predki, *Berechnung von Schneckenflankengeometrien verschiedener Schneckentypen*, Antriebstechnik - Organ der Forschungsvereinigung Antriebstechnik e.V. Heft 2/85, Frankfurt/Main (1985)
4. DIN 3975-1, *Begriffe und Bestimmungsgrößen für Zylinder-Schneckengetriebe mit sich rechtwinklig kreuzenden Achsen-Teil 1: Schnecke und Schneckenrad*, Beuth Verlag, Berlin, (2017)

The vehicle that can move on an accidental field

CÂRJALI EROL
Universitatea OVIDIUS Constanta
Romania

Abstract: *The designed vehicle can move on rough terrain (with multiple bumps); also (the vehicle) can climb a sloping terrain (with a relatively large angle).*

The movement (of the vehicle) is not continuous; contact with the ground (tread) takes place periodically, simulating the steps taken by a moving man; this movement is obtained by generating a hypocycloid.

The vehicle will move with the help of four wheels; they (wheels) will lift and move the vehicle when they come in contact with the road (ground).

1. Introduction

Off-road vehicles are able to travel on rough terrain. Their purpose (of off-road vehicles) is to transport materials and people in difficult conditions [2].

Off-road vehicles can use large tires (diameter and width), tracks or combinations thereof (Fig. 1, 2).

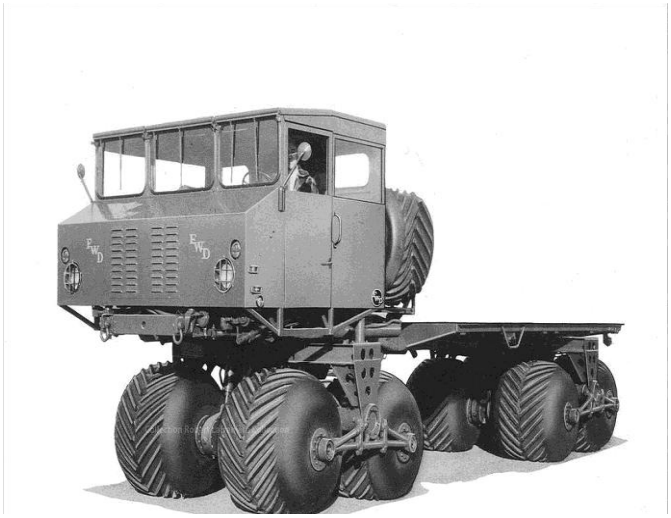


Fig. 1



Fig. 2

The vehicle presented in this paper uses a hypocycloid curve in combination with a chain drive.

2. General aspects

The hypocycloid is the curve described by a point on a non-slip circle, on a fixed circle; the small circle runs inside the large circle.

The landmark xOy is chosen, consisting of two parameters of the fixed circle of center O, so that the axis Ox passes through point A, initial point of contact between the circles in question (fig. 3) [3]. Consider rolling the center circle O 'from position A to an arbitrary position, with N the point of contact between the fixed circle and the moving circle. Point A will move to point M.

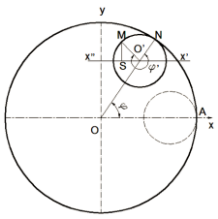


Fig. 3

Note:

$$\varphi = NOx, \quad \varphi' = MO'N, \tag{1}$$

in trigonometric sense and we obtain:

$$AN = MN, \tag{2}$$

(în sens trigonometric), adică:

$$a\varphi = b\varphi', \tag{3}$$

where from:

$$\varphi' = \frac{a}{b}\varphi \tag{4}$$

such as:
relationship that will be
used in the following

$$\varphi' - \varphi = \frac{a-b}{b}\varphi, \tag{5}$$

From the triangle OO'M we obtain:

$$\overline{OM} = \overline{OO'} + \overline{O'M}, \tag{6}$$

which results in:

$$\begin{aligned} x &= pr_{Ox}\overline{OO'} + pr_{Ox}\overline{O'M}; \\ y &= pr_{Oy}\overline{OO'} + pr_{Oy}\overline{O'M}. \end{aligned} \tag{7}$$

But

$$\begin{aligned} pr_{Ox}\overline{OO'} &= \overline{OO'}\cdot i = (a-b)\cos\varphi; \\ pr_{Oy}\overline{OO'} &= \overline{OO'}\cdot j = (a-b)\sin\varphi; \end{aligned} \tag{8}$$

$$pr_{Ox}\overline{O'M} = \overline{O'S}\cdot i = b\cos MO'x'' = -b\cos(\varphi' - \varphi - 180) = \quad (9)$$

$$= -b\cos(\varphi' - \varphi) = -b\cos\frac{a-b}{b}\varphi;$$

In geometry, a hypocycloid is a flat curve drawn by a point fixed on a circle that rolls inside another larger circle. It is similar to a cycloid, where the circle rolls on a straight line.

If the smaller circle has radius r and the larger circle has radius then the parametric equations for the curve are given by [5]:

$$x(\theta) = r(k-1)\left[\cos\theta + \frac{\cos(k-1)\theta}{k-1}\right]; \quad (10)$$

$$y(\theta) = r(k-1)\left[\sin\theta - \frac{\sin(k-1)\theta}{k-1}\right].$$

If k is integer, then the curve is closed and has k cupside.

If k is a rational number, then the curve has p cupside.

If k is an irrational number, then the curve never closes and fills the space in the large circle except for a radius disk in the center of the large circle.

A hypocycloid with three cupids is called a detoid.

A hypocycloid with four cupids is called an astroid.

Chain transmissions are indirect mechanical transmissions (via the chain); they transmit the motion (and torque) between two or more parallel shafts.

The principle diagram of the chain transmissions is presented in figure 4 (1 - driving wheel; 2 - driven wheel; 3 - chain); In addition to these elements (1, 2 and 3), chain drives may have tensioning devices, lubrication devices, as well as chain housings or guards [3].

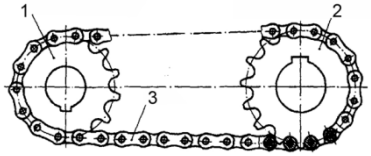


Fig. 4

The gear is the mechanism consisting of two gears, which transmit the rotational movement and torque between two shafts, through the teeth that are successively and continuously in contact (gearing).

3. Presentation of the device

The vehicle (fig. 5) is equipped with an internal combustion engine and two gearboxes that transmit through the four intermittent couplings, movements for the four satellite supports (fig. 6), which in turn transmit motion to the four hypocycloid transmissions (fig7) [1, 4].

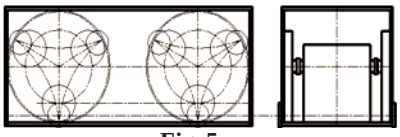


Fig. 5

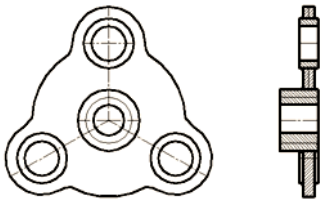


Fig. 6

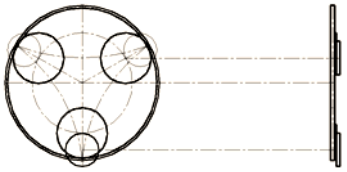


Fig. 7

The hypocycloid transmission (fig. 5) is composed of a toothed crown and a running system.

The running system (fig. 8) together with the toothed crown, imparts to the wheel of motion a displacement after a hypocycloid curve. Moreover, the drive wheel also has a rotation about its own axis, received through a chain drive.

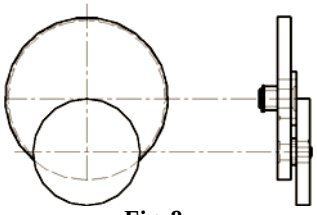


Fig. 8

The vehicle is designed so that the four wheels of movement come into contact with the ground (the road) in turn (for a short time, what will be the calculation below).

The vehicle moves using hypocycloid curves on the four motion systems.

Considering $R = 90mm$ and $r = 30mm$, results $k = \frac{90mm}{30mm}; k = 3.$

$$x_{(0^0)} = r(k-1)\left[\cos\theta + \frac{\cos(k-1)\theta}{2}\right] = 30mm(3-1)\left[\cos 0^0 + \frac{\cos(3-1)0^0}{2}\right] =$$

$$= 30mm \cdot 2\left(1 + \frac{1}{2}\right) = 90mm;$$

$$x_{(90^0)} = r(k-1)\left[\cos\theta + \frac{\cos(k-1)\theta}{2}\right] = 30mm(3-1)\left[\cos 90^0 + \frac{\cos(3-1)90^0}{2}\right] =$$

$$= 30mm \cdot 2\left(0 - \frac{1}{2}\right) = -30mm;$$

$$x_{(180^0)} = r(k-1)\left[\cos\theta + \frac{\cos(k-1)\theta}{2}\right] = 30mm(3-1)\left[\cos 180^0 + \frac{\cos(3-1)180^0}{2}\right] =$$

$$= 30mm \cdot 2\left(-1 + \frac{1}{2}\right) = -30mm;$$

$$y_{(0^0)} = r(k-1)\left[\sin\theta - \frac{\sin(k-1)\theta}{2}\right] = 30mm(3-1)\left[\sin 0^0 - \frac{\sin(3-1)0^0}{2}\right] =$$

$$= 30mm \cdot 2(0-0) = 0mm;$$

$$y_{(90^0)} = r(k-1)\left[\sin\theta - \frac{\sin(k-1)\theta}{2}\right] = 30mm(3-1)\left[\sin 90^0 + \frac{\sin(3-1)90^0}{2}\right] =$$

$$= 30mm \cdot 2(1-0) = 60mm;$$

$$y_{(180^0)} = r(k-1)\left[\sin\theta - \frac{\sin(k-1)\theta}{2}\right] = 30mm(3-1)\left[\sin 180^0 - \frac{\sin(3-1)180^0}{2}\right] =$$

$$= 30mm \cdot 2(0-0) = 0mm$$

For the initial point $(\varphi = 0)$, the quotas are $x = 90mm$ and $y = 0\ mm$ (see figure 3).

In figure 3 it is observed that for $R = a = 90mm$ and $r = b = 30mm$, when rotating at an angle it $\varphi = 90^o$, is obtained:

• the length of the arc on the radius circle $R = a = 90mm$, is:

$$l_{90^o a} = \frac{2\pi a}{360^o} \cdot 90^o = \frac{2\pi \cdot 90mm}{360^o} \cdot 90^o = 45\pi mm$$

• the rotation angle for the small, radius circle is $r = b = 30mm$, obtained with the relation:

$$l_{90^o b} = \frac{2\pi b}{360^o} \cdot \varphi' = 45\pi \ mm,$$

where from

$$\varphi' = \frac{360^o \cdot 45\pi}{2\pi \cdot 30} = 270^o.$$

Next, determine the position of the M point by rotating the small circle with $\varphi' = 270^o$ (where $\varphi = 90^o$).

$$pr_{Ox}\overline{O'M} \cdot i = -O'S = -b\cos MO'x' = -b\cos\left(\varphi' - \varphi - 180^o\right) =$$
$$= b\cos\left(\varphi' - \varphi\right) = b\cos\left(\frac{a}{b}\varphi - \varphi\right) = b\cos\frac{a-b}{b}\varphi =$$
$$= 30mm \cdot \cos\frac{90mm - 30mm}{30mm} \cdot 90^o = 30mm \cdot \cos 180^o =$$
$$= -30mm.$$
$$pr_{Ox}O' = p_{Ox}\overline{O'O} \cdot i = O'O\cos\varphi = (90mm - 30mm)\cos 90^o = 0$$

Point M is located on the Ox axis, at elevation:
$-30mm + 0 = -30mm.$

$$pr_{Oy}\overline{O'M} \cdot j = SM = b\sin MO'x' = b\sin\left(\varphi' - \varphi - 180^o\right) =$$
$$= b\sin\left(\varphi' - \varphi\right) = b\sin\left(\frac{a}{b}\varphi - \varphi\right) = b\sin\frac{a-b}{b}\varphi =$$
$$= 30mm \cdot \sin\frac{90mm - 30mm}{30mm} \cdot 90^o = 0 \ mm.$$
$$pr_{Oy}O' = pr_{Oy}\overline{OO} \cdot j = O'O\sin\varphi = (90mm - 30mm)\sin 90^o =$$
$$= 60mm$$

Point M is located on the Oy axis at elevation:
$60mm + 0mm = 60mm.$
It is observed that the quotas are respected.

In figure 3 it is observed that for $R = a = 90mm$ and $r = b = 30mm$, when rotating at an angle it is obtained:

• the length of the arc on the radius circle $R = a = 90mm$, is:

$$l_{180^o a} = \frac{2\pi a}{360^o} \cdot 180^o = \frac{2\pi \cdot 90mm}{360^o} \cdot 180^o = 90\pi mm;$$

• the rotation angle for the small, radius circle is $r = b = 30mm$, obtained with the relation:

$$l_{180^o b} = \frac{2\pi b}{360^o} \cdot \varphi' = 90\pi \ mm,$$

where from

$$\varphi' = \frac{360^o \cdot 90\pi}{2\pi \cdot 30} = 540^o.$$

Next, determine the position of the M point by rotating the small circle with $\varphi' = 540^o$ (where $\varphi = 180^o$).

$$pr_{Ox}\overline{O'M} \cdot i = -O'S = -b\cos MO'x' = -b\cos\left(\varphi' - \varphi - 180^o\right) =$$
$$= b\cos\left(\varphi' - \varphi\right) = b\cos\left(\frac{a}{b}\varphi - \varphi\right) = b\cos\frac{a-b}{b}\varphi =$$
$$= 30mm \cdot \cos\frac{90mm - 30mm}{30mm} \cdot 180^o = 30mm \cdot \cos 360^o =$$
$$= 30mm.$$
$$pr_{Ox}O' = p_{Ox}\overline{O'O} \cdot i = O'O\cos\varphi = (90mm - 30mm)\cos 180^o = -60mm.$$

Point M is located on the Ox axis, at elevation:
$-60mm + 30mm = -30mm.$

$$pr_{Oy}\overline{O'M} \cdot j = SM = b\sin MO'x' = b\sin\left(\varphi' - \varphi - 180^o\right) =$$
$$= b\sin\left(\varphi' - \varphi\right) = b\sin\left(\frac{a}{b}\varphi - \varphi\right) = b\sin\frac{a-b}{b}\varphi =$$
$$= 30mm \cdot \sin\frac{90mm - 30mm}{30mm} \cdot 180^o = 0 \ mm.$$
$$pr_{Oy}O' = pr_{Oy}\overline{O'O} \cdot j = O'O\sin\varphi = (90mm - 30mm)\sin 180^o =$$
$$= 0mm.$$

Point M is located on the Oy axis at elevation:
$0mm + 0mm = 0mm.$
It is observed that the quotas are respected.

The following is the calculation of the vehicle movement.

Figure 7 shows that the vertical displacement is 25 mm.

Calculate the angle at which the wheel of motion comes into contact with the ground (tread):

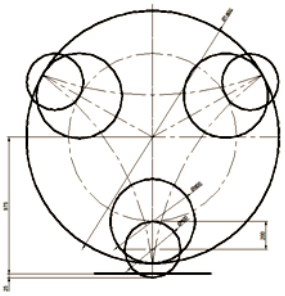
$$\cos\varphi = \frac{175mm}{200mm} = 0,875 \Rightarrow \varphi = 28,9^o \ \square \ 29^o \Rightarrow 2\varphi = 58^o.$$

Consider the speed of the satellite support $n_1 = 10\frac{rot}{min}$. The speed of the satellite wheels will be $n_2 = 10\frac{rot}{min} \cdot 3 = 30\frac{rot}{min}$.

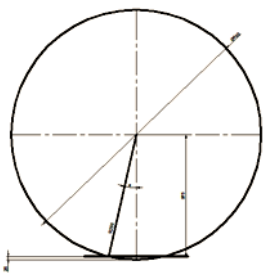
The movement is transmitted through the chain, with a ratio of 2, ie the speed of the movement wheel is $n_3 = 60\frac{rot}{min}$.

Approximating the contact time of the wheel of motion with the ground (running path), we obtain:

$$t = \frac{1s}{\frac{360^o}{58^o}} \ \square \ \frac{1s}{6,2} = 0,161s.$$



a



b

Fig. 9

The peripheral speed of the wheel of movement is:
$v = \pi \cdot 400mm \cdot 60\frac{rot}{min} = \pi \cdot 400mm \cdot 1\frac{rot}{s} = 1256\frac{mm}{s}$. Moving the device to a wheel contact is $s = 0,161s \cdot 1256\frac{mm}{s} = 202,31mm.$

If the movement wheels are offset, which can be obtained during assembly, the displacement with the four wheels will be four times greater than 0.161 s, ie: $S = 202,31mm \cdot 4 = 809,24mm$.

4. Conclusions

The vehicle can travel on rough terrain. If the movement wheels are equipped with "sticking" elements (in the form of cones or pyramids) the possibility of slipping is eliminated.This vehicle can also be used on a stepped road, adapted (the road) to the possibilities of the road system or the road system can be adapted to the existing conditions in the field.

References

1. Cârjali E., Organe de mașini, vol. 3, Editura Ovidius Universiti Press, Constanța 2010
2. Sârbu L, Utilaje de ridicat și transportat pentru construcții, montaj industrial și căi de comunicații în transporturi, Editura MATRIX ROM, București, 2019
3. Chiriacescu S, Dinamica mașinilor și uneltelor. Prolegomene, Editura Tehnică, București, 2004
4. Frățilă Gh., Calculul și construcția autovehiculelor, Editura Didactică și Pedagogică, București, 1984
5. Analiză matematică

Determination of the quality of welds produced by robotic welding

Janette Brezinová[1], Ján Hašul'[1,*], Jakub Brezina[1]
Department of Technology, Materials and Computer Supported Production, Technical University of Košice, Slovakia[1]
jan.hasul@tuke.sk, janette.brezinova@tuke.sk

Abstract: *The paper focuses on the evaluation of the quality of fillet welds produced robotically by the method of impulse synergic welding MAG. This welding technology is used in the automotive industry in the production of rear seat backs for passenger cars. In the process of automated production, the speed of the process, accuracy, and quality of the made joints are important. Several factors affect the accuracy and quality of welded joints. The paper presents the results of research where the influence of filleting of fillet welds on their quality was confirmed. Visual and capillary methods were used to determine the quality of welds, metallographic analysis for evaluation depth of weld root penetration, strength properties of welds were evaluated by static tensile test. Statistical ANOVA methods were used to process the obtained values. Experimental work confirmed that the depth of welding of the weld root into the base material has the greatest influence on the final quality of fillet welds. It is this parameter that results in the elimination of the weld and thus the entire product.*
Keywords*: WELDING, AUTOMOTIVE, ROBOTIZATION, DEFECTS, ROOT WELD, ANOVA*

1. Introduction

The automotive industry struggles continuously with the need to increase competitiveness and profitability. Due to their structural importance, metallic components and systems represent a major part of the weight of an automobile. These metal components are connected by different technologies to create multiple subsets, to get the final product. Therefore, several sets of metallic components need to connect [1].

Welding is a joining process used to join two materials (usual metals) by controlled coalescence of temperature and pressure. There are many types of welding process developed for various applications. Ensuring the weld quality with minimal cost and time is of great importance in a manufacturing industry [1,2]. MAG/MIG, TIG, submerged Arc and laser welding processes are those more commonly used in industrial applications [1,2]. It is known that the welded joint of two components is the most susceptible zone to initiate fatigue crack, significantly reducing the component lifetimes [2]. In several cases, those welded connections are subjected to repeated loading, which may lead to fatigue failure, mainly high cycle fatigue regime, associated with many loading cycles. Fatigue is the result of regular or irregular cyclic stresses imposed on the component, that may lead to fatigue cracks initially microscopic, that propagate to visible cracks, leading to the rupture of the component [2]. Residual stresses along the welded joint imposed by heating and cooling cycles may cause a decrease of the fatigue life of welded components. The weld joint geometry also has an important effect on the fatigue life of the structure. A defective weld geometry may also increase tensions in the welded joint. Weld joint geometry depends on the process and the operation parameters (the welding energy, welding speed, voltage, electric current, wire feed speed). In the MAG process, the welding speed and energy are lower than those used on the laser process. Thus, higher base material dilution, penetration and arear of the heat affected zone can be expected. However, concentration of residual stresses also increases [2].

Welding quality can be improved by proper welding automation with aid of robots and online monitoring mechanisms. Automated robotic welding is commonly used for the joining of thin sheet metals for automotive industry due to the precision and speed of the welding process. Without proper process optimization, high speed robotic welding for automotive industry is known to have defects, such as porosity, weld concavity and cyclic humping. Several welding parameters can be adjusted to optimize the robotic welding is decreasing the welding speed, changing the intensity distribution of the heat on the surface of the substrate, changing the type and flow rate of shielding gas used during welding process etc. However, decreasing these parameters leads to a loss in productivity which can be costly in large scale manufacturing endeavors [2,3]. Along with the development of social productivity and the progress of science and technology, welding robots are more and more widely used in a industrial production. Welding robots can not only greatly improve the production efficiency and quality, but also can greatly reduce the amount of labor and reduce the technical requirements on the operation of workers. They have the advantages of stability, high repetition accuracy etc. Robotic autonomous welding is one of the key technologies in intelligent welding manufacturing [1-4]. In the jointing of thick plates, such as shipbuilding and pressure vessels, multi-pass robotic welding has the advantages of high welding efficiency and quality and has been widely used to reduce the heavy labor caused by large numbers of welds. However, due to the thermal deformation or the assembly error, the teach-playback welding robots cannot adapt to the variation in welding trajectory, which leads to the decrease of welding quality [5]. Therefore, the vision sensor-based welding seam tracking is urgently needed to realize intelligent zed robotic multi-pass welding. Robotization, automation and digitalization will be the important development direction of welding process, and the research of seam tracking has become on of the significant research field of welding equipments [6].

1.2 Defects of welded joints

With increasing requirement of service reliability, some key components call for higher mechanical performance, especially the fatigue reliability and corrosion resistance for the welded structure [7]. The fatigue mechanism of the metallic components with welded joints is an important scientific issue, because welding process can cause an obvious loss of fatigue strength [8]. For the metallic component, the fatigue crack often initiates from the site that suffer a high stress concentration, and therefore the fatigue crack usually starts from the weld toe of the welded metallic component, at which the change of weld surface geometry causes obvious stress concentration. Slag inclusion, porosity, inhomogeneous microstructure, and various cracks are some typical defects, that are unavoidably formed in the welding process [8-12].

According to the ISO 6520-1 standard, we recognize two main groups of welded joint defects [9,10]:

1. **Internal defects**, which include an overheated root, unboiled root, shrinkage, and others

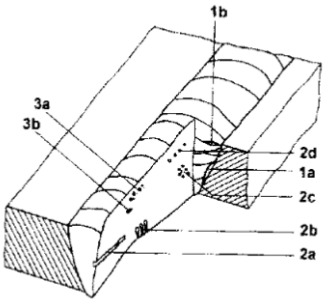


Fig. 1 *Internal defects of welds*

2. **External (surface) defects**, which include cracks, cavities, inclusions, cold joints and non-penetrations, longitudinal cracks in the weld metal, resp. in the base material, metal spatter and other

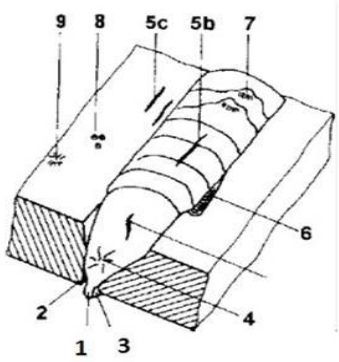


Fig. 2 *External defects of welds*

2. Materials and Methods

In the automotive industry, profiles are used for the rear seat backs, which have a closed square profile measuring 25.4 mm in two-phase cold-rolled steel with a thickness of 1.3 mm. Two-phase ferritic-marensitic steel HCT 590X was used in the analyzed nodes. The European designation of this steel is EN 10338. The chemical composition as well as the mechanical properties of HCT 590X are given in Tab. 1 and. Tab.2.

Table 1: *Chemical composition of HCT 590X*

Element	C	Si	Mn	P	S	Al	Cr+Mo	Nb+Ti	V	B
Weight [%]	0.15	0.75	2.5	0.04	0.015	1.5	1.4	0.15	0.2	0.005

Table 2: *Mechanical properties of HCT 590X*

Tensile strength [MPa]	590
Yield strength [MPa]	550
Ductility [%]	12

Welds in the analyzed nodes were created robotically by MAG pulse synergic welding technology. CO_2 working gas and inert (protective) gas Ar in the ratio CO_2 / Ar = 82% / 18% were used. G3Si1 welding wire with a diameter of Φ 1.0 mm intended for welding fine-grained steels with a minimum Re up to 470 MPa was used as an additional material for all types of welds. The chemical composition of the additional material is given in Tab. 3.

Table *3: Chemical composition of the G3Si1 additive material*

Element	C	Mn	Si	Fe
Weight %	0.07	1.4	0.85	-

The parameters of the welding process are given in Tab. 4 and the monitored parameters of fillet welds are shown in Fig.3:

Table *4: Parameters of MAG welding*

Voltage [V]	Current [A]	Gas consumption [l/min]	Wire feed speed [m/min]	Welding power [kg/h]	Weld metal recovery [g/100g]
18-32	80-300	18	2.7-15.0	1.0-5.6	96

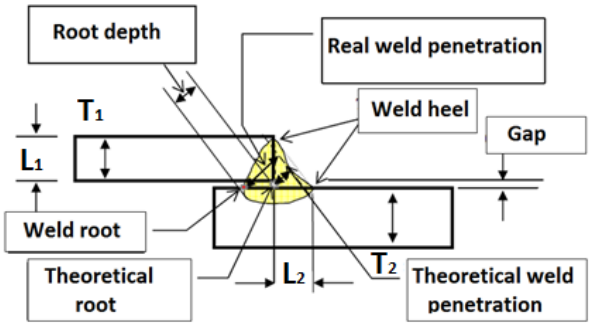


Fig. 3 *Monitored parameters of fillet welds*

The welding torch (Fig.4) is located on a robotic arm, which contains a feeder for feeding and removing wire of additional material.



Fig. 4 *Welding torch on a robotic arm with automatic feed slider*

The tested weld nodes on the car seat frame formed by MAG robotic welding are shown in Fig.5. Visual control according to ISO 17637 and NDT capillary test according to ISO 23277 were used to evaluate welded joints. Microhardness was measured by the Vickers method according to ISO 9015-2. A modified static tensile test according to ISO 6892-1 was designed to determine the strength of welds. The static tensile test was performed on a TIRATEST 2300 device.

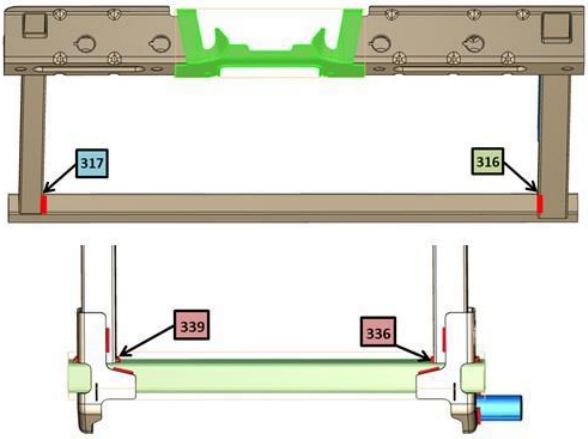


Fig. 5 *The tested weld nodes*

3. Results and discussion

3.1 Strength of fillet welds

Two types of jigs were designed for the modified static tensile test. In the case of the first jigs (Fig.6), the vertical part of the sample was clamped using mechanical forceps. After starting the test, the sample was released. This problem was solved by welding a steel sheet to the vertical surface of the sample. Nevertheless, there was till a very strong deformation.

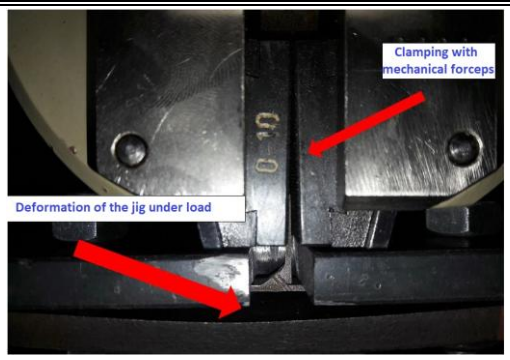


Fig. 6 *Sample in the mechanical forceps*

The second type of jig (Fig.7) was designed to hold the sample with hydraulic forceps, thus ensuring a firm grip on the vertical part of the sample. The sample was deformed even with this type of jig and the subsequent loading.

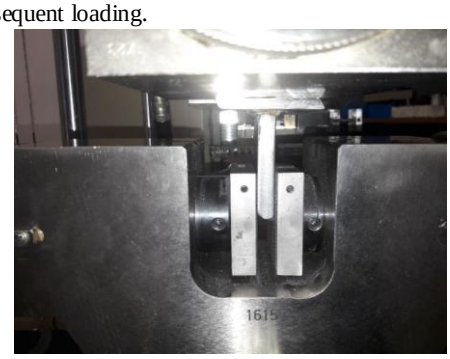


Fig. 7 *Sample in the hydraulic forceps*

3.2 Microhardness of fillet welds

In terms of microhardness, similar values were achieved due to the use of the same production technology and the additional materials. However, slightly higher values were found for the weld metal compared to the base material. The microhardness values for the base material are given in Tab.5:

Table *5:* Microhardness of basic material

	Microhardness values HV 0,1					**AVERAGE**
Basic material	293	234	213	240	245	**245**

The minimum and maximum values of HV0.1 for individual weld nodes were measured:

- ✓ For weld node 316 Hv_{min} = 270, resp. HV_{max} = 308
- ✓ For weld node 317 HV_{min} = 216, resp. HV_{max} = 333
- ✓ For weld node 336 HV_{min} = 201, resp. HV_{max} = 212
- ✓ For weld node 339 HV_{min} = 242, resp. HV_{max} = 262

3.3 Metallographic analysis of fillet welds

The basic monitored parameter was the depth of the root boiling, which had to reach values in the range of 0 to 0.14 mm. In addition to welding errors such as inflammation in the material, the depth of root boiling proved to be a crucial parameter in evaluating the quality of welds. The depth of boiling of the root into the base material was the only parameter that showed regular deviations from the allowable values. In Fig. 8 is shown a weld, that did not exceed any of the limits in Tab.6, so it can be marked as a suitable weld (Fig.8a) and the unsatisfactory weld (Fig.8b) due to inflammation in the material, where the measured value was 0.31 and the limit tolerance of weld errors is 0.26 from Tab.6:

Table *6: Limit tolerances of weld errors*

	Weld nodes							
	316		317		336		339	
	Min.	Max.	Min.	Max.	Min.	Max.	Min.	Max.
Boiling the root (mm)	0.13	0	0.13	0	0.14	0	0.14	0
Inflammation in the material 1 (mm)	0	0.26	0	0.27	0	0.28	0	0.28
Inflammation in the material 2 (mm)	0	0.26	0	0.27	0	0.28	0	0.28
Porosity (mm)	0	0.53	0	0.54	0	0.55	0	0.57

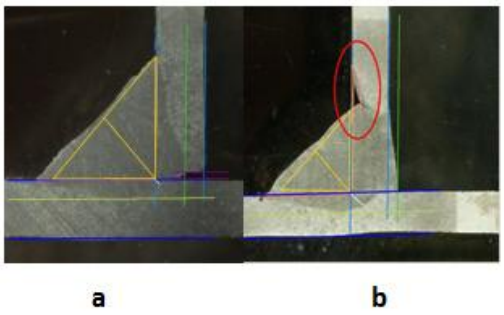


Fig. 8 *Suitable weld (a), unsatisfactory weld – inflammation in the material (b) – weld node 316*

3.4 Statistical analysis of fillet welds

The number of welds in individual tested weld nodes, which were in the normal tolerance value of welds for the monitored parameter of root depth boiling are given in Tab.7:

Table *7*: Number of welds in the standard

Weld nodes				
	316	317	336	339
Number of weld in the standard	34	36	35	36
	25	24	25	27
Percentage [%]	**73.5**	**66.7**	**71.4**	**75**

A graph (Fig.9) was the constructed from the measured values, which shows and describes the average values of the monitored parameter (root welds), the range of measured values for individual weld nodes and their standard deviations. The ANOVA statistical tool used the F test to verify the null hypothesis H0. It is true that we reject H0 if $F \leq \alpha$; $\alpha = 0{,}05$. Significance of F test the weld nodes addiction to parameters Z_1, Z_2 and L_1, L_2 is shown in Tab.8:

Table *8*: ANOVA – level of significance

Weld nodes	**Significance F - test**	
	Addiction to Z_1 a Z_2	Addiction to L_1 a L_2
316	0.0137	0.0468
317	0.1047	0.9616
336	0.0012	0.9328
339	0.3002	0.1080

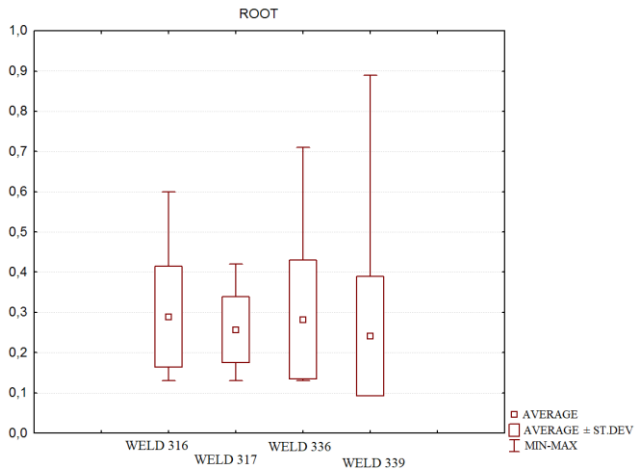


Fig. 9 *Graph of average values of weld nodes*

4. Conclusions

The paper is the result of research into the evaluation of fillet welds created robotically by the MAG welding method. The basic material was two-phase ferritic-martensitic steel HCT 590X. The work methodology included destructive and non-destructive methods of measuring the quality of welds. Visual and capillary methods did not identify any non-compliant welds. The microhardness evaluation did not show any difference between the hardness of the base material and the weld metal of the individual welds with respect to the same welding parameters. Using an optical microscope, 25 samples from each weld node were analysed separately by metallographic analysis. The total number of samples was 100 pieces. A total of 26 pieces were determined for faulty connections. The resulting weld quality was assessed based on the depth of root penetration in the base material. Experimental work has confirmed that the quality of fillet welds is affected by the depth of root penetration into the base material. This parameter effect can be caused by several factors:

- Incorrect position of the welding torch
- Incorrect trajectory of the welding torch
- Dimensional tolerances of input components

5. Acknowledgments

This contribution is the result of the project implementation: “Innovative approaches to the restoration of functional surfaces by laser weld overlaying” (APVV-20-0303), supported by the Slovak Research and Development Agency and supported by the Ministry of Education of Slovakia Foundation under grant projects VEGA No. 1/0497/20 “Application of progressive technologies in restoration of functional surfaces of products” and KEGA 046TUKE-4/2022 “Innovations of the educational process by implementing adaptive hypermedia systems in the teaching of subjects in the field of coating technology and welding of materials“. This support is highly appreciated by the authors. Conflicts of Interest: The authors declare no conflict of interest.

6. References

1. M. Dourado et.al.: A comparative study of fatigue behaviour of MAG and laser welded components using reliability analysis, Materials Science & Engineering 2014, Vol. 606, pp. 31-39

2. R. Sachin et.al.: Study of Mechanical Properties and Weldability of Aluminium Alloy and Stainless steel by Gas Metal Arc Welding, Materials Today: Proceedings 2020, Vol. 24, pp.1167-1173

3. A. Sumesh et.al.: Establishing Correlation Between Current and Voltage Signatures of the Arc and Weld Defect in GMAW process, Arab. J. Scie. Eng., 2017, Vol. 42, pp. 4649-4665

4. M. Shehryar Khan et.al.: Numerical modelling and experiment validation of the effect of laser beam defocusing on process optimization during fiber laser welding of automotive press-hardened steels, Journal of Manufacturing Processes 2021, Vol. 64, pp.535-544

5. R. Xiao et. al.: A feature extraction algorithm based on improved Snake model for multi-pass seam tracking in robotic arc welding, Journal of Manufacturing Processes, 2021, Vol. 72, pp. 48-60

6. Kunxi Xue et. al.: Robotic seam tracking system based on vision sensing and human machine interaction for multi-pass MAG welding, Journal of Manufacturing Processes 2021, Vol. 63, pp. 48-59

7. V. Knysh et.al.: Influence of hardening by high-frequency mechanical impacts of butt-welded joints made of 15KhSND steel on their atmospheric corrosion and fatigue fracture resistace, Materials Science, 2018, Vol.54, pp. 1-9

8. H. Polezhayeva et.al.: Fatigue performance of friction stir welded marine grade steel, Int. J. Fatigue, 2015, Vol. 81, pp. 162-170

9. Peter Babčanský: Determination of the quality of fillet welds in the automotive industry, Diploma thesis, 2019

10. H. Yamamoto et.al.: Weld toe modifications using spherical-tip WC tool FSP in fatigue strength improvement of high-strength low-alloy steel joints, Mater. Des., 2018, Vol. 160, pp. 1019-1028

11. W. Ting, W. Dongpo, H. Lixing, Z. Yufeng: Discussion on fatigue design of welded joints enhanced by ultrasonic peening treatment (UPT), In: Int. J. Fatigue, 2009, Volume 31, pp. 644-650

12. Y. Sakino, Y. Sano, R. Sumiya, Y.C. Kim: Major factor causing improvement in fatigue strength of butt-welded steel joints after laser peening without coating, In: Sci. Technol. Weld. Join., 2012, Volume 17, pp. 402-407

Research on loading-transport machine parts in order to determine the causes of defects

Rositsa Gavrilova, Boyan Yordanov, Dimitar Krastev, Iliyan Mitov
University of Chemical Technology and metallurgy, Sofia, Bulgaria
E-mail: r.gavrilova@abv.bg

Abstract: *Possible defects in the system: piston-cooling jacket occur for various reasons. This system work in severe conditions: heat load; variable gas pressure and mechanical friction, which requires high strength, good wear resistance with limited lubrication and overall high resistance to abrasion, corrosion and other wear.The operation of the cylinder-piston group with insufficient or poor quality oil is the most common cause of overheating or engine blockage. Seizing of one or more pistons leads to major engine repairs or even scrapping. Damaged fuel injectors, inaccurate injection or ignition timing can also cause the mechanism to melt or puncture. Therefore, it is essential to identify the exact causes of defects in the system and look for ways to prevent them.*
Studied details were functioned under the identical conditions of good lubrication and no overheating. The reason, apart from the ones mentioned above, which led to their destruction, has been established.
KEYWORDS*: LOADING MACHINEs, SEIZED PISTONS, DEFECTS*

1.Introduction

The wear of the cylinders of automobile engines is a consequence of the complex action of many physical and chemical fast-moving processes, and most often it is the result of three main types of impacts:

- erosion impact, due to mechanical friction, abrasion and other destructive processes as a result of direct contact with friction metal surfaces;
- corrosion effects, caused by various oxidative processes on friction surfaces;
- abrasive impact, caused by the destruction of friction surfaces by solid particles between them.

Each of the listed effects, as well as the combination of them, can be the cause of defects. A common reason for the appearance of defects is the type of material from which the individual parts of the engine are made. These materials and them behavior is subjected to this paper, including the following methods of research: Chemical analysis; Macrostructural and Microstructural metallographic analysis; Hardness measurement.

2. Preconditions and means for resolving the problem

2.1. Theoretical Model

During operation of the engine, the pistons may break due to forced overload, foreign body colliding with the piston or fatigue of the material, shown in Fig.1:
Forced fracture is always caused by a foreign body colliding with the piston while the engine is running. These foreign bodies can be torn off parts of the connecting rod, crankshaft, valves and more. Forced piston breakage can also occur if water or fuel enters the cylinder and results in hydraulic shock. The fracture surfaces of such a fracture appear gray. They do not show wear and deformation lines. The piston breaks suddenly.

Fig 1 *Examples of piston breakage caused by various factors*



a

a) Fracture caused by a foreign body



b

b) Fracture due to fatigue of material

In case of fatigue breakage of the material, deformation lines are formed on the surface, which reveal the beginning and progressive trend of the fracture. Fracture surfaces often wear to the point of being extremely smooth and looking shiny. The cause of metal fatigue breakage is overvoltage of the piston
A defect can occur due to:

- detonation combustion;
- strong vibrations of the piston if its forehead has mechanical contact with the cylinder head;
- defects in the material of which the piston is made;
- Excessive piston clearance.

Excessive deformation of the piston bolt due to overstrain (bending and radial deformation) causes cracks in its hole. In addition, fatigue fractures can also be caused by cracks from overheating the piston forehead. The figure shows the fracture of the piston in the holes for the piston bolt.

Fig 2 *Example of piston breakage caused by fracture of the piston in the holes for the piston bolt*



2.2. Experimental stand. Examination of pistons – original piston, non-seized piston and seized pistons

The chemical composition of material from which the pistons are made is given in Table 1. The equipment is from the BRUKER AXS Company, Germany.

Table 1 *Chemical composition of piston samples*

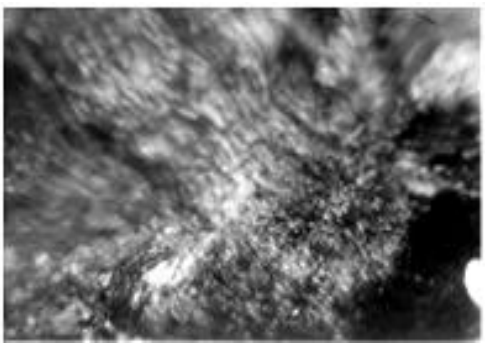
Chemical composition, %	Original piston	Non-seized piston	Seized piston 1	Seized piston 2
Cu %	1,33	1,21	1,25	1,22
Mg %	1,02	1,07	1,12	0,96
Si %	18,67	17,00	17,25	17,03
Fe %	0,71	0,49	0,69	0,41
Mn %	0,20	0,16	0,22	0,20
Ni %	0,88	0,80	0,71	0,92
Zn %	0,08	0,15	0,11	0,07
Ti %	0,09	0,09	0,10	0,10
Cr %	0,08	0,02	0,06	0,03
Al %	The percentage complements up to 100%			

The obtained data show that the material is silumin - AlSi18CuNiMg, [1, 2]. All three pistons are in the brand according to Bulgarian State Standard 12223-74, as in the seized and non-seized pistons Si is at the lower limit of 17.03 and 17%, respectively, and in the original piston is 18.67%.
The composition of these alloys shows, that they are multicomponent systems, based on the elements Al-Cu-Mg and with added Si, Ni, Mn and other elements. Mn and impurities of iron and silicon are obligatory in these alloys. The main components providing the strengthening of the alloys are Cu and Mg. Manganese is a must-have additive because its presence helps to crush the structure, increase strength and corrosion resistance. As additional elements available, Fe and Si are unavoidable in these alloys. Iron appears as a harmful impurity that reduces their strength and ductility. Silicon to some extent compensates for the harmful effects of iron by binding it in a phase, more easily destructible in plastic deformation [2÷6].

2.1.1. Macrostructural metallographic analysis

The conducted macrostructural analysis includes examination of the place of "dragging", seizing of the piston, which was destroyed as a result of the appearance and development of this defect. This section was taken at magnifications of 150x and 500x, the photos are shown in Fig. 3.

Fig. 3 *Occurrence and development of seizing defect, led to destruction of the material*



a

Magnification 150x



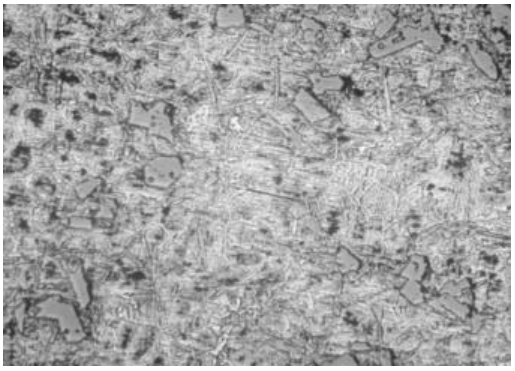
b

Magnification 500x

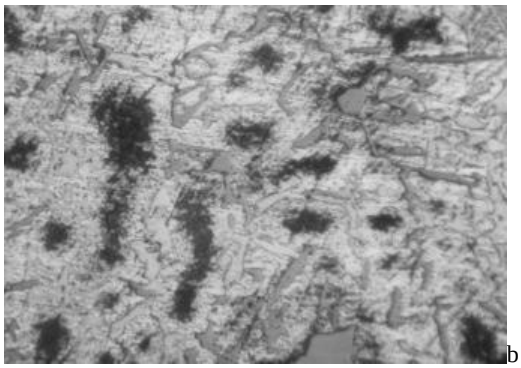
2.1.2. Microstructural metallographic analysis of piston samples

The microstructural analysis was performed after fabrication and preparation of metallographic sections according to standard methods. The structure was observed on a metallographic microscope MIM 8 with a digital camera, the micrographs were taken at magnifications of 240x and 360x. Some of them are shown in Fig. 4÷6.
The structure of the original piston is fine with an even distribution of the primary Si crystals. In the defective seized piston the inhomogeneity and much coarser structure are obvious. Accumulations of Si crystals up to 2-3 times larger than those in the original, were observed.
The structural elements, described above, are presented at fig. 4 to the original piston; fig. 5, to the non-seized piston and at Fig. 6, for the seized pistons at the same magnification. Rough separations, with uneven distribution in the matrix structure and sharp edges, under load could become stress concentrators and be a good reason for the initial "dragging", seizing of the detail and subsequent destruction.

Fig. 4 *Original piston*
a) Magnification 240x; b) Magnification 360x;

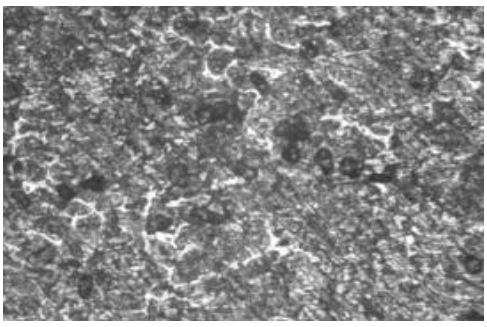


a



b

Fig. 5 *Non-seized piston*
a) Magnification 240x; b) Magnification 360x;



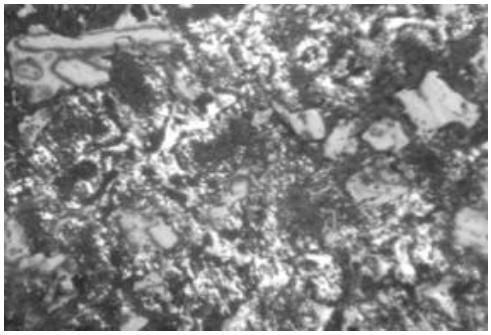
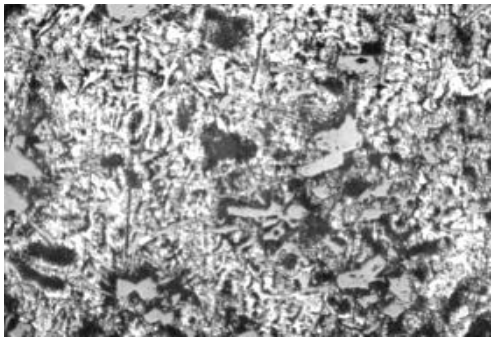
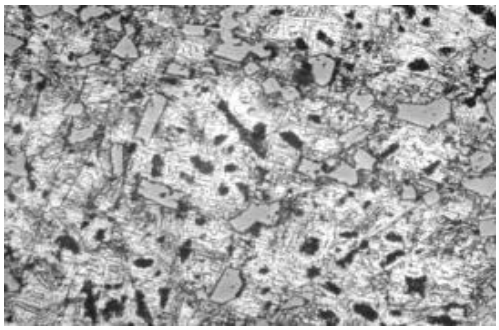
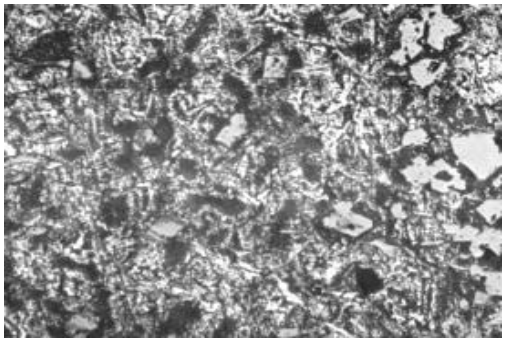
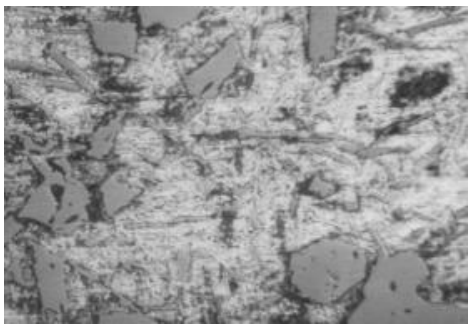


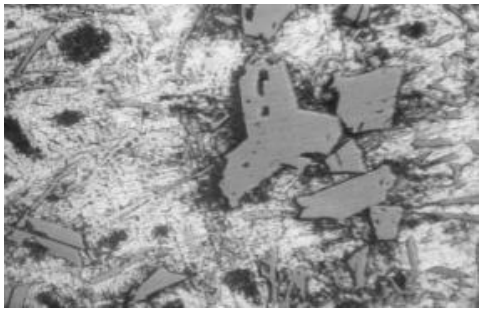
Fig. 6 *Seized piston*
a,b,c) Magnification 240x; d,e,f) Magnification 360x;

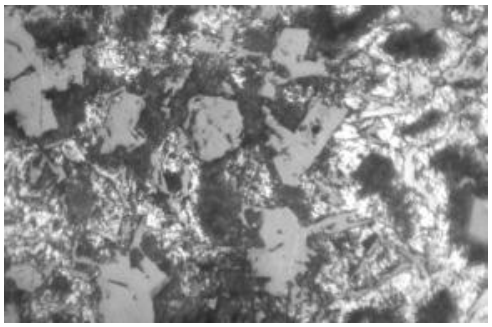

a


b


c


d


e


f

In the microstructure of the piston, which worked in the engine for the same period of time and at a similar load, structural inhomogeneity is also observed, but to a lesser extent.

2.1.3. Measurement of hardness of test specimens

Brinell hardness was measured on a Brinell-Rockwell equipment at a test load F=125 [kgf] and a penetrating sphere diameter D=5mm. Arithmetic mean values of 5 pieces were obtained, [3]. Measurements are shown in Table 2.

Table 2 *Hardness measurement*

Original piston	≅118HB
Non-seized pistons	≅100HB
Seized pistons	Values from 88 to 130 HB have been calculated, depending on the measurement location;

The hardness of the three pistons meets the requirements of Bulgarian State Standard 12223-74, as the different, lower values in the seized piston can be explained by the heterogeneity of the structure.

3. Results and discussion

It is impossible to give an unambiguous answer as to how long the mechanism will last and whether the piston will not show a purely operational defect, a defect as a result of incorrectly performed production process or a defect of poorly selected material for its manufacture.

Based on the comparative analysis of the original, seized and non-seized pistons, the following conclusions were made:

In practice, the piston cylinders operate in identical modes. The normal operating temperature of the silumin piston fronts is not more than 250°C. In more severe operating conditions, if overheating is allowed, the material with inhomogeneous structure expands differently in the areas with accumulations and large separations from those with a relatively balanced structure. The high coefficient of linear expansion in the working piston leads to stresses where inhomogeneous areas have already occurred during the casting process, [5]. Due to the small distance between the piston, the segments and the cylinder liner, the piston inflated by thermal and structural stresses touches its walls. A “drag effect” is observed, [4,6÷8].

4. Conclusion

The macrostructural analysis of the place of destruction showed that the appearance and growth of the defect until its destruction is of mixed type - in certain areas it is fragile, in neighboring - plastic. The metal fracture visually looks like "twisted", probably the origin of the definition "dragged" piston is due to this type.

Microstructural analysis of the samples of original and seized pistons shows differences in the structure, mainly in the size and distribution of silicon emissions, namely:

- The original piston has a fine structure with small single formations. Unsuccessful modifications and omissions in the casting technology are the most probable reason for the presence of coarse Si crystals in the seized piston. The structure of the non- seized piston is close to that of the seized piston, but is characterized by smaller sizes of Si-crystals releases and uniform distribution.
- Equivalent and approximately equal in size grains are observed in the original piston. Areas with very large grains and others with very small ones are observed in the defective one. A similar effect could be obtained as a result of poorly performed or no homogenizing annealing, which would achieve a balanced internal crystal structure and good ductility of the cast metal.

This gives us reason to conclude that the detail was destroyed as a result of a technological rather than an operational defect.

5. References

1. http://www.splav-kharkov.com/z_mat_type.php
2. Anchev V., Physical Metallurgy, part I, Sofia, Technical University, 1990.
3. Laboratory Workshop on Metallurgy, Krastev, Yordanov, Gavrilova, Klyavkov, Lazarova, 2020, ISBN 978-954-465-108-4 9
4. BSS 2734-83 Tensile/compression material testing.
5. BSS 5177-05 Defects in castings. Terminology and classification of defects, Sofia, 1986.
6. Handbook of Metallurgy and Metal Processing by Plastic Deformation, Acad. Marin Drinov, Union of Metallurgists in Bulgaria, 2009.
7. Maneva, Stanev, Details of aluminum alloys for the automotive industry, Proceedings of "FOUNDRY 2014", 196-199, ISSN 1310-3946.
8. Stanev, Iotov, Comparative study of the behavior of dry and abrasive friction and wear of a piston aluminum alloy, Proceedings of "FOUNDRY 2014", 200-203, ISSN 1310-3946.

Influencing factors on the speed of vehicles in the school and kindergarten zones on the territory of Novi Sad

Milja Simeunović, Zoran Papić, Nenad Saulić
Faculty of Technical Sciences – University of Novi Sad, Novi Sad, Serbia
mlekovic@uns.ac.rs.

Abstract: *Pedestrians, in addition to cyclists, represent the most vulnerable road users. Children from an early age participate in traffic as pedestrians, so the need to increase their level of safety is understandable. The speed limit in a school and kindergarten zones, by installing different types of calming measures, is one of the measures applied to protect children in traffic. It often happens that despite the speed limit and placement of speed humps on the roads, drivers do not respect the speed of movement and move at a much higher speed than allowed. Within this work, the speed of vehicles in the zones of some schools and kindergartens in the area of Novi Sad was measured. Based on the obtained results, factors that have an impact on the regime of vehicle movement in the investigated areas have been identified.*

Keywords: SHOOL AND KINDERGARTEN ZONES, CALMING MEASURES, SPEEDING

1. Introduction

Children from the earliest age participate in traffic. Their inexperience and the role they play in traffic make them the most vulnerable road users. The safety of this category of road users is a great challenge for experts dealing with these problems. In recent years, there has been a growing trend in the number of road traffic accidents in Serbia. Comparing the number of fatalities per million inhabitants in Serbia and other European Union countries, it can be seen that Serbia is among the last few countries [1]. The number of children in road traffic accidents is not negligible. About 32% of the total child fatalities in road traffic accidents are pedestrians. The largest number of pedestrian children died in the cities (97%), of which 86% of children fatalities outside intersections. As many as 20% of children fatalities, and 24% of children were injured at the pedestrian crossing [2]. All these indicators show that it is necessary to take maximum care of the safety of children in populated areas. The highest concentration of children is in the kindergarten and school zones, where preschool children generally do not participate in traffic on their own. Therefore, various technical and regulatory measures are most often applied in these zones, which increase the safety of pedestrians.

2. Traffic regulation in school/kindergarten zones

The application of technical and regulatory measures is necessary in areas of intensive pedestrian flows, especially children. Certain measures are applied to prevent pedestrians from improperly using traffic areas intended for the movement of vehicles. Other measures are aimed at warning motor vehicle drivers to enter the zone of increased concentration of pedestrians. In Serbia, some of the measures have been implemented in school zones are prescribed by law.

According to Article 163 of the Law on Traffic Safety, it is envisaged that the school zone is marked with appropriate traffic signals, that the traffic experts take appropriate measures to increase child safety and that the speed of vehicles is limited to 30 km/h in populated areas and 50 km/h outside populated areas in the period from 07 to 21 h [3]. Limit the speed of vehicles are usually implemented by applying traffic signs and setting different types of calming measures. By applying various measures to slow down traffic, the speed of vehicles is reduced and the level of safety of all road users is increased. At low speeds, if necessary, drivers have a greater opportunities of avoiding a car accident.

Despite all the measures that are taken in school zones, it often happens that drivers do not respect the set restrictions. Within this paper, the research was performed, which included measuring the vehicle speeds in the school and kindergarten zones. The aim of the research was to determine the effect of the applied measures in these zones and to possibly determine the factors that influenced the speeding.

3. Research methodology

The research was conducted in the area of Novi Sad, at selected locations in the primary school and kindergarten zones. A total of 20 locations were selected. During the research, an analysis of all selected locations was performed. By visiting each individual location, data on traffic signals, calming measures on the road and the organization of parking in the area of schools and kindergartens were recorded. In addition, vehicle speeds were measured. Vehicle speeds were measured by the Bushnell Velocity Speed Gun Detector (Figure 1), which has a speed measurement range of 16-322 km/h. At a distance of 25-450 m, the maximum value of the measurement error is 1 mph. Speeds of those vehicles that were less than 16 km/h and could not be detected by radar were recorded as speeds of 15 km/h.



Fig. 1 *Bushnell Velocity Speed Gun Detector*

3.1. Research results

By analyzing the selected locations, it was determined that the following traffic signals were installed at all locations in primary school zones: pavement marking V-15.1 "SCHOOL" and traffic signs III-28 "school zone" and III-28.1 "end of school zone". Traffic sign I-15 "children on the road" have been set up in the kindergarten zones, which, among other things, indicate the proximity of the kindergarten.



Fig. 2 *Pavement marking "SCHOOL"*



Fig. 3 *Traffic signs III-28 "school zone" i III-28.1 "end of school zone"*



Fig. 4 *Traffic sign "children on the road"*

The organization of parking at the researched locations can also influence on the traffic flow and vehicle speed, so that the existence of parking lots in the school and kindergarten zones has been recorded. It often happens that vehicles are parked on the street when children arriving or leaving school/kindergarten, which causes traffic congestions, so recording was not done during these periods.

Table 1 shows the results of the survey, for each individual location, giving data about the number of lanes in the street where the school / kindergarten is located, the existence of parking in the observed street, the existence of calming measures on the road, as well as measured vehicle speeds (minimum speed, maximum speed and average speed).

By analyzing the data, it was determined that the speeds at the observed locations range from 16 km/h to 70 km/h. The law defined that the speed for school zones in populated areas is limited to 30 km/h. The measurement results show that most vehicles at the observed locations had a speed higher than 30 km/h. This is the best illustrated in Figure 5. Figure 5 shows the share of measured vehicle speeds exceeding 30 km/h of the total number of measured speeds, observed by locations. At a quarter of the observed locations, all measured speeds were higher than 30 km/h, while at only one location all measured speeds were below 30 km/h.

Table 1 *Research results*

Location	Number of traffic lines	Parking	Calming measures	Min. speed	Max. speed	Aver. speed
PS 1	2	yes	yes	22	42	29
PS 2	4	yes	yes	27	49	39
PS 3	2	no	yes	16	30	20
PS 4	4	no	no	31	57	45
PS 5	2	yes	yes	18	51	29
PS 6	2	yes	yes	20	39	26
PS 7	6	no	no	44	65	54
PS 8	2	no	yes	22	65	39
PS 9	1	yes	yes	18	41	30
PS 10	2	yes	yes	24	39	30
K 1	2	no	no	19	37	28
K 2	2	no	yes	23	38	30
K 3	2	yes	yes	36	47	39
K 4	1	yes	no	20	34	27
K 5	2	no	yes	32	49	40
K 6	2	yes	no	32	70	43
K 7	2	yes	no	21	62	41
K 8	2	yes	yes	18	47	28
K 9	4	yes	yes	28	47	37
K 10	2	yes	yes	18	33	25

Note: (PS – primary school; K – kindergarten)

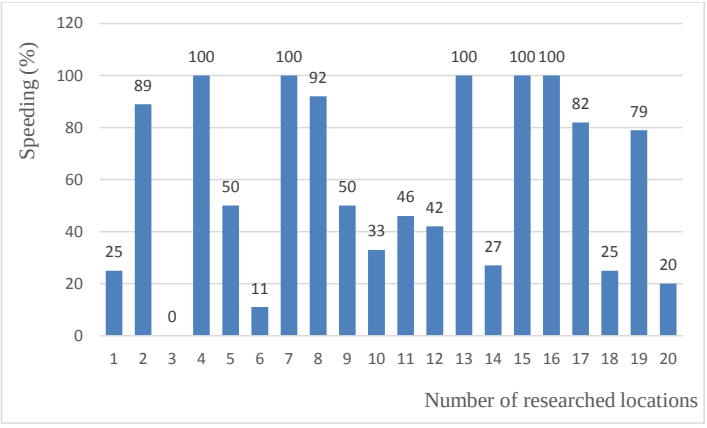


Fig. 5 *Participation of measured speeds over 30 km/h in the total number of measured speeds (%)*

The analysis of the locations with the highest number of measured speeding, concludes that the highest number of speeding was recorded on the primary street network, ie on the main city roads. On the roads with a large number of traffic lanes and where no calming measures were installed (locations 4 and 7), all measured speeds were over 30 km/h. The highest average speeds were recorded at these two locations. The share of speeding on the secondary street network is significantly lower. The lowest speeds were measured at location 3, which is expected because it is a dead end street.

3. Conclusion

The road safety of children must be a high priority for traffic safety experts and other road users. It is necessary to constantly work on improving the measures that are being implemented. First of all, it is necessary to design a set of preventive measures, and only after that should repressive measures be carry out. The research conducted in this paper shows that most drivers do not respect the set signalization and speed limits that are set in the school and kindergarten zones. Speeding in zones where no calming measures is significantly more pronounced than in zones where calming measures exist. In the zones with calming measures, even at 65% of the locations, the average speed was up to 30 km/h. The class of street in the road network also has a significant influence on the measured speeds.

4. References

[1] Agencija za bezbednost saobraćaja (2020), Statistički izveštaj o stanju bezbednosti saobraćaja u Republici Srbiji u 2019. godini. https://www.abs.gov.rs/sr/analize-i-istrazivanja/statistika-i-analize/statisticki-izvestaji (27.04.2022.)

[2] Agencija za bezbednost saobraćaja, Pregledni izveštaj, Bezbednost pešaka u saobraćaju, 2021 https://www.abs.gov.rs/admin/upload/documents/20211221085112-pesaci_pregledni_2018_2020.pdf (27.04.2022.)

[3]https://www.paragraf.rs/propisi/zakon_o_bezbednosti_saobracaja_na_putevima.html (13.05.2022.)

Use of innovative methods in the management of tourist transport infrastructure

Gvantsa Arjevanidze, Nargiza Karkashadze, Tinatin Gugeshashvili, Izolda Dangadze,
Akaki Tsereteli State University, Kutaisi, Georgia
Gvantsa.arjevanidze@atsu.edu.ge , Nargiza.karkashadze@atsu.edu.ge , Tinatin.gugeshashvili@atsu.edu.ge , Izolda.dangadze@atsu.edu.ge

Abstract: *In many countries in the world, including Georgia, tourism has become one of the leading sectors of the country's economy and a source of raising public finance. Tourism is recognized as one of the priority areas for the development of the Georgian economy and contributes to the socio-economic development of the country. In particular, it is important to explore the existing tourism transport infrastructure and introduce the innovative technologies in its management. The paper describes some innovative methods whose use will contribute to the development of tourism in Georgia and will significantly increase the attraction of visitors.*
Keywords*:TOURISM INDUSTRY, TOURISM INFRASTRUCTURE MANAGEMENT, TOURIST ATTRACTIONS, TOURIST CLUSTER.*

1. Introduction

Georgia, with its geopolitical location and existing natural, historical or cultural resources, has tremendous opportunities for tourism development. A comparison of the growth rates of the world and Georgia in the tourism sector shows that in the last five years the number of travelers in Georgia has been growing at a much faster pace than in the world, with the exception of the pandemic period. The international tourism market is one of the key components of Georgia's economic growth. The share of transport services in the overall structure of tourism services is more than 40%. Today, when tourism is recognized as one of the priority areas of economic development of Georgia, and it contributes to the country's socio-economic development, it is especially important to study the existing tourism transport infrastructure and introduce innovative technologies in its management.

2. Preconditions and means for resolving the problem

Market signals at the current stage of tourism development are characterized by several groups of parameters as follows:

1. Economico:
   - o Economic growth and integration;
   - o Raising the level of economic development of the regions;
   - o Increased investment in the tourism industry;
   - o Raising the level of infrastructure development of the country;
   - o Hypercompetition.
2. Political:
   - o Development of state and regional tourism policy;
   - o Simplification of tourist formalities;
   - o The impact of political events on tourism demand.
3. Sociocultural:
   - o Changing lifestyles;
   - o Increased demand for tourism services;
   - o Raising the tourists' demands;
   - o Increasing travel accessibility and raising population mobility;
   - o Development of information and communication technology.
4. Industry group:
   - o Development of consolidation and integration processes;
   - o Development of new tourist destinations;
   - o Development of a range of tourism services;
   - o Changing the forms of customer relationship;
   - o Increasing the impact of the sector on the economy.

These parameters influence the management methods used in the current practice of tourism management in Georgia. Today, strategic, conceptual and program-targeted approaches are most often used in management. The results of applying these approaches are the targeted programs, strategies and concepts for the development of regions and cities, as well as sectoral visions and strategies. The target-oriented approach is relatively new. Among these there are programs of scientific and technical, economic, social, regional, and environmental orientation. The target-oriented method of management is widely used today, however, it has a number of significant drawbacks, namely:

1. Methodological incompleteness (researchers have no a common point of view on the basic concepts of target-oriented planning and management, the ratio of the plan and target complex program; this method is used in most cases to improve the existing management systems);
2. Low cohesion of control systems with the problems for which they are created;
3. Lack of methods for calculating the economic efficiency of programs;
4. Low efficiency in solving the problems set by the program;
5. Lack of responsibility for the results of the programs.

These shortcomings fully applicable to programs built using the target-oriented approach; in addition, the lack of an integration approach in them can be distinguished. For example, "Development of domestic tourism in Georgia and "Development of domestic and inbound tourism in Georgia" indicate the dependence of tourism on the development of transport and engineering networks, the development of certain types of transport and the effectiveness of their management. However, the programs for the development of certain types of transport, transport strategies, the visions for the development of certain areas of the transport industry do not take into account either the needs of the tourism industry or tourists, despite the ever-increasing influence of tourism on transport. Particular attention is paid to the development of tourism infrastructure. The program considers 3 possible scenarios for the development of domestic and inbound tourism:

1) Development of tourism infrastructure in all subjects, regardless of their economic development, infrastructure development and the level of tourism potential;

2) Development of tourism infrastructure for a limited number of subjects of Georgia, the most promising in terms of the development of domestic and inbound tourism;

3) Development of the most promising tourism infrastructure in terms of the development of domestic and inbound tourism using the cluster approach, as well as the implementation of projects directed at the accelerated development of interregional tourism opportunities and improving the quality of services.

The program selects the third scenario. As result of the implementation of the program activities, it is planned to create a network of modern resort and tourist facilities within the relevant

tourist, recreational and auto-tourist clusters that meet international standards and can significantly increase the competitiveness of the country's tourism services market. Why the auto-tourist clusters were chosen, and what they are? These clusters will become enlarged investment projects that provide for the creation and construction of new tourist facilities in limited areas provided with appropriate state support. The tourism cluster is a set of tourist and recreational special economic zones created by the decision of the Government of Georgia and located in one or more areas of the territory of Georgia and municipalities defined by the government. Special economic zones of tourist-recreational type represent another direction of tourism development management in Georgia. The creation of such zones has 2 goals:

1. To develop the existing resort areas
2. To attract investment to the region.

The mechanism for establishing special economic zone for tourism development is widely used in many countries.

Modern researchers of the transport industry name 5 main areas that can be attributed to the management of the development of tourism transport infrastructure services, namely: the development of transport infrastructure, the improvement of transport infrastructure management, the introduction of innovations in the field of transport infrastructure management, changing the role of government in the management of transport infrastructure and the work of non-governmental organizations and associations. Let us consider these areas in more detail.

1. Development of transport infrastructure through: -improving the road network; - traffic calming; - promotion of "smart driving"; - improvement of the regulatory and legal support of the transport industry;

2. improvement of transport infrastructure management through:

- management of traffic flows; - management of public transport; - use of a client-oriented approach; - organization of parking sites and lots;

- use of automated control systems (monitoring, video surveillance, automatic control systems, electronic payments).

3. Introduction of innovations in the field of transport infrastructure management through: -use of intelligent transport systems; - navigation and information services.

4. A change in the role of the state in the process of managing the development of transport infrastructure network is seen by theoreticians in the form of the development of various mechanisms of public-private partnership, which, unfortunately, do not work in Georgia to the full extent.

5. The work of non-governmental organizations and associations. Some researchers propose in their works the creation of a non-profit organization - an association of representatives of the tourism and transport sector, however, instead of integration, transport and tourism companies more often choose competition, penetrating into each other's business environment, creating subsidiary companies or departments engaged in transportation.

We have polled a staff employed in the field of tourism throughout Georgia, with the aim of identifying problems related to the transport services of tourists, which prevent tourism development. A total of 50 specialists in the field of tourism - aviation, rail, road transport (as the main form of transport in tourism) were interviewed. In the survey, which included an assessment of the level of development of tourism transport infrastructure in Georgia, the lowest score was 3 points (out of a maximum of 10 points) for bus stations and road infrastructure, followed by road infrastructure with 4 points, rail transport, road transport, railway stations and the level of service in transport (equal points (5 points each), the level of staff training in transport is slightly behind the level of training of specialists in tourism (difference is 1 point), the same and higher rates (7 points each) were obtained by airports and air transport. The service satisfaction level indicator in tourism rated 8 points. Overall, the specialists emphasized the low level of development of transport infrastructure in tourism in Georgia and the urgent need to undertake a number of state measures to radically change the inter-regional tourism opportunities and the quality of services.

A special role in the development and management of transport infrastructure in foreign countries is played by the state, which was originally the owner of major transport resources and remains the main investor in transport tourism infrastructure and is responsible for the strategic development of transport. In order to realize and effectively manage the country's transport potential, states use the following mechanisms:

1) Privatization or partial privatization of transport complex enterprises on the basis of concessions, lease agreements or other forms of public-private partnership in order to attract public investments;

2) Comprehensive state regulation and financing of the transport complex;

3) Attracting private companies to manage state property without the right of ownership being transferred to them.

4) A combination of several options.

The popularity of urban passenger transport among the population varies from country to country: in the US it accounts for 15-20% of total travel, in Japan and France - 20-30%, in the UK and Germany - 30-40%, in Russia – more than 75% [Stephen J. 2009. 447], but tourists very often use urban passenger transport while staying in another country. However, every country and not every city can offer tourists convenient travel schemes, comfortable and safe transportation, interesting routes. The awareness of tourists about the local transport system and effective management plays an important role in this. In developed countries, this sector is actively developing deregulation, privatization and reduction of state subsidies, in order to gradually move to covering the operating costs of urban passenger transport, not from the state budget, but from the local budget. In countries that are leaders in terms of tourism competitiveness and tourist infrastructure development, government subsidies to cover the operating costs of transport reduced to zero. At the same time, the government maintains the relevant legislative regulation of transport activities of administrative, control and supervisory nature. The main trends in the management of tourism transport infrastructure in developed countries are as follows:

- Demonopolization and privatization of transport enterprises;
- Modernization of the existing transport networks, increasing their capacity;
- Reducing the share of transport costs in the value of products and services;
- Development of the new modes of transport;
- Reducing the number of vehicles in large cities;
- The priority development of urban transport.

In developing countries, the main focus is on increasing transport capacity, rapid development of roads and railways, construction of airports, and development of local airlines. The main role of transport infrastructure has always been to ensure access to tourist destinations. At the same time, at this stage, the foreign experts in the planning and development programs of tourist areas are reassessing the transport infrastructure. The reassessment of the role of transport in tourism began in the late 1980s. It has been realized that the growing flows of tourists who have the opportunity to travel to almost any part of the world could cause irreparable damage to some areas and lead to the degradation of tourism resources [World Economic Forum. 2013].

There are three main strategies in the field of tourism transport management in developed foreign countries:

1. Measures to tighten the use of tourism resources, their fencing, traffic restriction and redistribution, promotion of the use of alternative means of transport.

2. Regulation of the use of territories by restricting/prohibiting entry from the territory zone, introduction of entrance fees (the most controversial option), use of special traffic schemes for visitors, management of public and private transport networks, speed limit, size of groups of visitors, characteristics of vehicles used, and marketing.

3. Establishing oversight of the location, scale, activities and type of tourism activities that affect traffic flows.

Strategies share similar objectives, but none of them are universal. There are several interstate partnerships dealing with the transportation of tourists, including: NETS, based on the Association for Sustainable Mobility, G.A.S.T. - Association of Car Free Tourist Destinations and IACF - Association of Car Free Tourist & Spa Destinations in Bavaria, MOST and others.

The foreign tourist centers address the problems of tourism transport infrastructure development in different ways. First of all, attention is paid to air transport, airlines, airports, because in many countries most of the visitors arrive to the country by air. In large countries and island states, regional and local aviation play an important role in transportation of travelers. Tourist buses, taxis, public transport are the main means of transporting them to the host country. Buses, trains, ferries, sea and river boats are used by tourists both for traveling between countries and for excursions. The tourism business of each country or region has a priority to develop a specific type of transport.

The United States and Canada have the most developed aviation and road (private and rental) transportation. The most developed network of rail and bus routes is also popular in Central European countries (Austria, Great Britain, Germany, Switzerland), as well as travel by car. In the Scandinavian countries and states that have islands, sea transport is in high demand. An example of an ideal tourist transport system is the Swiss transport system, which has created and is successfully operating the Swiss Travel System. A special advantage of the Swiss Travel System is the variety of travel documents. The Zurich Card is a ticket for all types of urban and suburban transport. At the same time a discount card, Swiss Pass, Swiss Youth Pass, Family Card and others are designed for different categories of travelers, combining the desire to see as much as possible and save money when ordering excursions. The permit is valid for the entire transport network. There is a huge tourist demand for the panoramic railway routes, of which Switzerland has the most: Glacier Express, Mont Blanc Express, Swiss Chocolate Train and others. A unique tourism product has been created based on the country's tourism transport infrastructure.

Tourists can find out more about travel system opportunities on the Internet and at tourist ticket offices at major stations and airports, as well as in travel companies around the world [Pender L. 2005; 322]. The foreign tourist centers have the opportunity to provide travelers with quality tourist transport services for the following reasons:

- All types of transport are well developed and coordinated, regardless of ownership form;
- Transport infrastructure facilities meet modern requirements for comfort and safety;
- A bilingual information environment is available to most visitors;
- Strategic planning of tourism and transport has been developed;
- Modern level of management of tourism and transport enterprises is provided;
- Marketing support for tourism and transport;
- Flexible price offers for different categories of tourists;
- Public transport priority is ensured;
- A stringent system of rules and fines in transport and parking areas;
- Methods are used to reduce congestion in historic centers, specially protected areas, highways and city streets (prohibition/restriction of entry) .

In addition to the above conditions, new programs are constantly being developed to improve the tourism transport infrastructure:

- Special bike trails have been arranged to improve the conditions for cycling;
- Great attention is paid to the promotion of ecological forms of transport.

The above approaches to tourism transport infrastructure management are mostly related to developed countries where transport and tourism infrastructure is well developed and provided with a high level of management.

The process of managing tourism transport infrastructure in developing countries has a slightly different vector of development, the aim of which is primarily to create transport infrastructure, and in the absence it, to develop new tourist destinations and attract the flow of tourists. In the Arab countries (United Arab Emirates, Qatar), the economy began to recover by shifting from the manufacturing sector to the service sector, with the creation of airlines and airports, the development of the country's transit capacity, and the promotion of the country as a tourist destination. China's economy defines tourism as a growth point for further economic growth, and transport infrastructure - as a means of its development.

3. Conclusion

When tourism is recognized as one of the priority areas for the development of the Georgian economy and contributes to the socio-economic development of the country, it is especially important:

1. To study the existing tourist transport infrastructure and to introduce innovative technologies in its management;

2. To work out the main directions for the development of tourism transport infrastructure in Georgia;

3. To identify the general problems of the regions in the development of tourism transport infrastructure.

4. References

1. Pender L., Sharpley R. The Management of Tourizm. London: SAGE Publications, 2005. – 323 p.
2. Sorupia E. Proceedings of the Eastern Asia Society for Transportation Studies, Vol. 5, pp. 1767 – 1777, 2005 [http://www.easts.info/online/proceedings 05/1767.pdf].
3. Stephen J. Page. Transport and tourism. Global perspectives. 3 rd edition, London: Pearson education Ltd. 2009. – 447 p.
4. The Travel & Tourism Competitiveness Report, World Economic Forum, 2008 [http://www.werforum.org/docs/WEF-TravelTourizmCompetitiveness-Report-2008.pdf].
5. The Travel & Tourism Competitiveness Report, World Economic Forum, 2009 [http://www3.werforum.org/docs/WEF-TravelTourizmCompetitiveness-Report-2009 pdf].
6. The Travel & Tourism Competitiveness Report, World Economic Forum, 2011 [http://www3.werforum.org/docs/WEF-TravelTourizmCompetitiveness-Report-2011 pdf].
7. The Travel & Tourism Competitiveness Report, World Economic Forum, 2013 [http://www3.werforum.org/docs/WEF-TravelTourizmCompetitiveness-Report-2013 pdf].

Decade of road markings and traffic signs quality testing in Croatia

Dario Babić.,[1], Mario Fiolić.[1], Goran Zovak.[2]
Faculty of transport and traffic sciences, Zagreb, Croatia[1]
Centar for vehicles of Croatia, Zagreb, Croatia[2]
dario.babic@fpz.unizg.hr
mario.fiolic@fpz.unizg.hr
goran.zovak@cvh.hr

Abstract: *With more than 1.35 million fatalities worldwide each year, road crashes are among the world's most significant public health and injury prevention problems. In the last decade, with the new technological breakthroughs, a significant effort has been devoted to improving different safety systems related to infrastructure and vehicles. Road marking and road signs represent main road elements whose main task is to provide timely and necessary information to the drivers related to the upcoming situation. In other words, they warn and inform drivers about the conditions and construction characteristics of the road, guide road users through the traffic network and regulate traffic in a safe way. Therefore, continuous monitoring and testing of their quality is of great importance for road safety in general. The aim of this paper is to present Croatian experience regarding the quality testing of road markings and signs in last decade. Overall, the analysis confirmed that systematic control of road markings and signs will positively affect their quality and optimize maintenance activities.*
Keywords*:* ROAD MARKINGS, ROAD SIGNS, QUALITY CONTROL, ASSET MANAGEMENT, MAINTENANCE

1. Introduction

When looking at the road infrastructure, road markings and traffic signs are an integral part of it and represent the basic means of communication between the relevant road authorities and road users. Based on their classification, i.e., meaning, the purpose of the road markings and traffic signs is to manage, regulate, inform, and warn road users to ensure their safe movement throughout the transport network. [1] Thus, they represent important road safety elements whose presence may influence road users in a positive way and increase overall road safety. [2]

Especially important role road markings and traffic signs play during conditions of reduced visibility in driver sees what the light from vehicles headlights lighten [3]. For road markings and traffic signs to be seen during such conditions, they must be retroreflective. Retroreflection is a measure of an object's ability to reflect light back towards a light source along the same axis from which it strikes the object [4]. Therefore, to ensure adequate retro reflectivity levels both road markings and traffic signs should be periodically checked. Several methods of quality control and maintenance are used in practice such as visual inspections, typical service life or different measurement methods. Overall, worn, damaged and/or insufficiently retroreflective road markings and traffic signs have shown to be an influential factor to occurrence of road accidents [5,6] during low visibility conditions.

Quality testing of road markings and traffic signs, according to EN 1436:2018 and EN 12899-1, includes various tests such as retroreflection and chromatic measurements, durability, resistance to weathering, accelerated natural weathering for traffic signs etc. Since in road traffic most decisions (90 %) are based on visual clues [7], form the safety point of view, the most important tests are those related to the visibility, i.e., retroreflection of road markings and traffic signs. Therefore, the aim of this paper is to present the impact of continuous control of road markings and traffic signs retroreflection on their long-term quality. The paper presents results of quality testing of road markings and traffic signs during last 10 years in the Republic of Croatia with analysis and conclusions of collected data.

2. Methods for quality control of road markings and traffic signs in Croatia

Measuring retroreflection of road markings and traffic signs give the road authorities an inside look at how road marking and traffic signs perform, in which condition they are, and how well conductors do their job. This section provides a basic description for quality control of road markings and traffic signs performed in the Republic of Croatia.

3.1. Road markings

Retroreflection measurement of road markings can be done in two ways: static or dynamic measuring method. Static method refers to the use of hand-held retro reflectometer which enables the measurement of daytime and night-time visibility. The daytime visibility (Qd) according to European Standard EN 1436:2018 (Materials for Road Markings – Characteristics) represents the road markings visibility observed at an angle of 2.29° at a distance of 30 m under diffuse light, while the night–time visibility or retroreflection (RL) represents the retroreflection of a light beam from the tested surface at an angle of 2.29°, with a light inlet angle of 1.24° and at a distance of 30 m with low–beam headlights on a vehicle. Both are expressed in mcd·m-2·lx-1.

Dynamic method includes the measurement of night-time visibility with dynamic retro reflectometer installed on the left or right side of measuring vehicle. The method allows continuous measurement of the night-time visibility of road markings while driving. Principle of measuring visibility at night with dynamic retro reflectometer is the same as in static measuring device. [8]

In the Republic of Croatia, the conducted tests ensure prescribed quality of road markings which comprise [9]:

- preliminary tests or convenience tests,
- routine tests,
- control tests,
- additional control tests,
- arbitration tests,
- tests prior to the expiry of the defect's liability period.

Convenience tests include tests aimed at proving the convenience or suitability of a material intended to be used for applying road markings, based on the foretold type of marking and prescribed quality. Ongoing tests, conducted by the Works Contractor, determine the prescribed quality of material, and works performance. The tests comprise testing of the thickness of wet and dry paint layer, testing daytime and night-time visibility in dry conditions, testing night-time visibility in wet conditions (only for type II road markings − road markings with special properties intended to enhance the retroreflection in wet or rainy conditions) and slip resistance.

Control tests, ensured by the Road Authority, determine whether the quality of the road markings system is compliant with the prescribed requirements. Mentioned tests comprise:

- control tests prior to the application of road markings which include identification, that is, verification of compliance (chemical and physical tests) between the delivered samples of the road markings material and the information presented in the certificates.

- control tests during the application of road markings, which include testing of the drying time, the thickness of wet and dry layer, the quantity of retroreflective material (glass beads) in the material and visual inspection of road markings.
- control tests applied on road markings, which include testing daytime and night-time visibility in dry conditions, testing night-time visibility in wet conditions (only for type II road markings) and slip resistance, as well as testing of the road markings geometry in terms of designed road markings width and length.

Additional control tests are conducted only if control tests on applied road markings resulted in limit values, while arbitrary tests involve repeating the control tests, if the Road Authority or the Contractor did not conduct the tests appropriately. An authorized legal entity which has not taken part in the disputed tests, or which has been approved by both parties conducts the tests to determine the quality of applied road markings and its compliance with the quality agreed for the duration of the warranty period.

4.2. Traffic signs

The coefficient of retroreflection of traffic signs (RA) is defined as the coefficient of luminous intensity of a plane retroreflecting surface to its area or as ratio od returned intensity to incident illumination divided by area of the retroreflector. The metric unit for retroreflection coefficient is cd·lx 1·m2. [10]

Retroreflection of traffic signs is measured by portable retro reflectometer containing an internal light source and a photoreceptor, and during the test they are placed on the surface of the sign to exclude the influence of daylight. Measurements with aforementioned device are performed according to European standards EN 12899-1: Fixed, vertical road traffic signs – Part 1: Permanent signs. Mentioned standard defines entrance and observation angles for different vehicle types and sign position. However common geometry implies an observation angle of 0.33° and entrance angle of 5°.

During the quality check, retroreflection of each colour on the traffic signs should be measured and comply the minimum retroreflection defined in the EN 12899-1 for RA1 and RA2, or in Consiglio nazionale delle ricerche: Common understanding of assessment procedure (CUAP): Microprismatic retro-reflective sheetings, 2002. for RA3 for the sign to be technically valid. The coefficient of retroreflection (RA) of all printed colours, except white, shall be not less than 70 % of the values defined in the EN 12899-1. [11]

3. Decade of road marking and traffic signs quality testing in Croatia

Department for Traffic Signaling at the Faculty of Transport and Traffic Sciences, University of Zagreb is conducting systematical measurements of road markings and traffic signs quality for over ten years on the roads in the Republic of Croatia. The department is an accredited testing laboratory (according to EN ISO/IEC 17025: 2017) for, among other, retroreflection measurements of road markings (both static and dynamic method) and traffic signs. To ensure the analysis of the conducted measurements, Department has developed softwares called *Retroreflection* and *SmartGis* where all the results from current and previous measurements are stored. Softwares also provides insight into detailed data about each road marking and traffic signs such as status, GPS coordinates, positions, type, materials, pictures etc. The following paragraphs will show the aforementioned measurement results in last 10 years in the Republic of Croatia.

3.1. Quality testing of road markings in Republic of Croatia

Control tests which determine whether the quality of the road markings system is compliant with the prescribed requirements are in Croatia conducted by a dynamic measuring device. The road markings are measured continuously within the measuring area and their average value is recorded for every 25, 50 or 100 meters, depending on the predefined settings. The measurements are conducted for two reasons: 1) with the aim of determining the road markings that need to be renewed (after winter period) and 2), after the renewal of the markings when it is necessary to carry out the control of the contractors. The aforementioned measurements have been conducted on state road and highways (both private and national).

3.1.1. State roads

Figure 1 shows map of all state roads in Republic of Croatia, which are, according to Croatian law, defined as important routes for road traffic between various parts of the country and as such represent secondary level roads (roads category below motorways). The length of state roads in Republic of Croatia is slightly longer than 7.307 km.



Fig. 1 *State roads in Croatia [13]*

Together with the state roads authority, measuring plans are developed each year depending on the maintenance priorities of road authority, their budget and road safety data. Table 1 shows measurements that were part of long-term check plan in Croatia.

From the table it can be concluded that in ten-year period (from 2010-2020) a total of 99.846 km of road markings was measured. There has been a total of 63.995 km of new lines (contractor control) and a total of 35.851 existing lines that were measured. All these measurements have been conducted to complete quality control plane made from Croatian Roads and creating a master plan to achieve visibility with minimal cost of renewal.

Table 1: *Total number of measured kilometers of road markings on state roads in Croatia*

Period	Total measured kilometers		
	Total (km)	New lines (km)	Existing lines (km)
2010-2011	14.096	9.614	4.482
2011-2012	17.918	8.372	9.546
2013-2014	13.591	9.354	4.237
2015-2016	23.377	17.414	5.963
2017-2018	10.453	7.394	3.059
2018-2019	10.043	4.262	5.781
2019-2020	10.368	7.585	2.783
Total	99.846	63.995	35.851

Overall, when looking at the average values of retroreflection of all measured renewed markings on state roads in Croatia (Figure 2), it can be noticed that values increased each year during the last decade. Although the average values each year increased by few percentages, the overall increase from 2010 to 2020 is around 13 %.

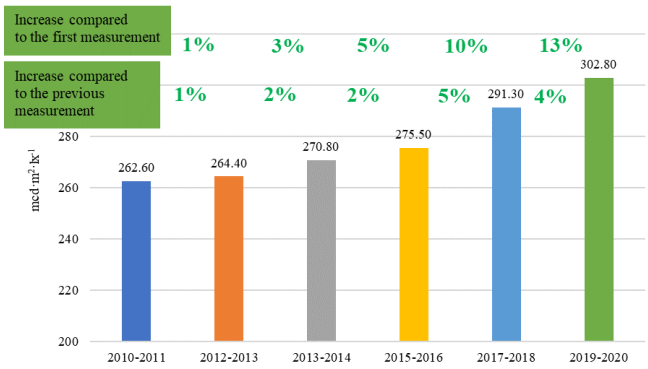


Fig. 2 *Average value of retroreflection of road marking on all state roads by year*

3.1.2. Motorways

Motorways in Croatia are the main transport network in Croatia. There are three network operators of which two are founded by government and one by joint venture. Operator BINA Istra oversees motorways A8, A9 (142 km), Highway Zagreb-Macelj (AZM) is in charge for highway A2 (62 km), and Croatian motorways (HAC) are in charge for A1, A3, A4, A5, A6, A7, A10 and A11 (1219 km). The motorway network of Republic of Croatia is presented in the Figure 3.



Fig. 3 *Motorways in Croatia [13]*

Table 2 shows conducted measurements on motorways in Croatia during a ten-year period. From below, it can be seen a systematical increase in total number of measured kilometers, as well as involved motorways. Unlike state roads, motorways under jurisdiction of HAC, were not measured systematically and continuously. On the other hand, motorway A2 (AZM) was measured systematically since 2013, as shown in Table 2. For this reason, below will be presented data obtained by measuring road markings on highway A2 (AZM).

Table 2: *Total number of measured kilometers of road markings on motorways in Croatia*

Period	Total measured kilometers on motorways in Croatia	
	HAC	AZM
2011-2012	5.217 km	
2013-2015		663 km
2016-2018		707 km
2019-2020	19.408 km	709 km
Total	26.705 km	

Average value of retroreflection on new road marking on motorways under the jurisdiction of AZM (Highway A2) at first two years was 296 mcd·m2·lx-1, in following two years was 358.5 mcd·m2·lx-1, and during last two years was 429.5 mcd·m2·lx-1 which indicates 17 % increase and 16 % within the observed period (Figure 4).

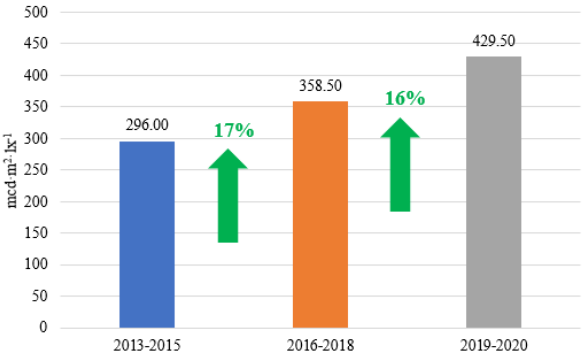


Fig. 4 *Average value of retroreflection on highway A2 (AZM)*

3.2. Quality testing of traffic signs in Republic of Croatia

As mentioned earlier, retroreflection of traffic signs is measured using handheld retroreflectometer device in accordance with the European and National standards and specifications. Expect the retroreflection, technical characteristic such as height, distance from the edge, compliance of signs with Regulations, etc. are also analysed. Measurements in state roads and motorways were carried out with the aim of creating a database of traffic signs, determining quality of traffic signs and with the aim of determining the priority of maintenance, i.e., replacement of dings that do not meet the prescribed criteria.

3.2.1. State roads

As mentioned earlier the length of state roads in Republic of Croatia is slightly longer than 7.307 km. In period 2013. – 2020. a total of 150.981 traffic signs have been measured and collected. Quality testing of traffic signs was conducted at 6.954,238 km, which represent 97 % of all state roads in the Republic Croatia. In total of 150.981 traffic signs that are collected, 27.428 traffic signs are warning sings, 38.787 are mandatory sings, 42.257 are information signs, 7.828 are guidance signs, 9.217 are additional panels, 24.042 are classified as road equipment and 1.235 are without code (**Грешка! Източникът на препратката не е намерен.**5).

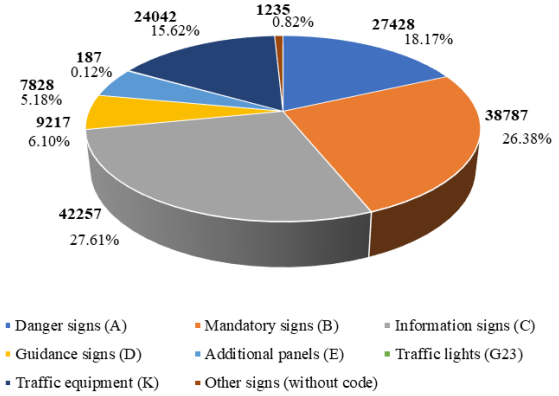


Fig. 5 *Total number of analyzed traffic signs classified by meaning on state roads*

The analysis of the retroreflection material from which traffic signs are made, showed that 99.576 signs are made from class I, 40.943 from class II and 10.462 from class III (Figure 6).

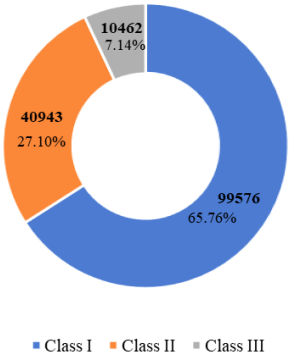


Fig. 6 *Total number of analyzed traffic signs classified by class of retroreflective material on state roads*

As year of production and implementation was recorded during the quality control, the average age of traffic signs was calculated. As shown from the Figure 7, average age of class I signs was 8.08 years, class II 6.87 years, and class III 5.67 years. In total, average age of traffic signs on Croatia state roads is 7.54 years.

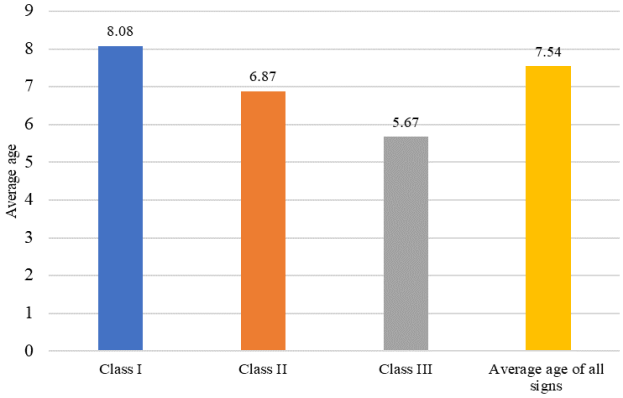


Fig. 7 *Average age of traffic signs by class of retroreflective material (years) on state roads*

Total percentage of traffic signs classified by class of retroreflection material that meet or do not meet the minimum value of retroreflection which can be seen from the Figure 7. From the Figure 8 out of 99.576 signs made of class I, 75.722 of them meet minimum retroreflection values. From 40.942 signs made of class II material, 32.455 of them meet the minimum values. Also, 12.318 traffic signs made of class III meet the minimum values.

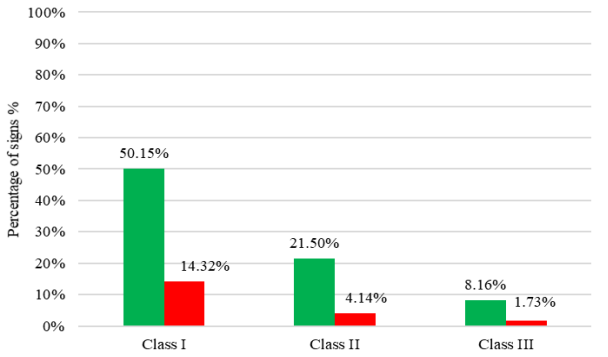


Fig. 8 *Total percentage of traffic signs by the class of retroreflective material that meet and do not meet minimum retroreflection values on state roads*

3.2.2. Motorways

There is a total amount of 8.257 traffic signs on motorways under jurisdiction of HAC in Croatia. By that means that on motorways A1, A3, A4, A5, A10 and A11, out of total traffic signs, the most numerous are of information signs (C) with percentage of 35.25 %. Following are mandatory signs (31.20 %), guidance signs (14.06 %), additional panels (7.79 %) etc. (Figure 9).

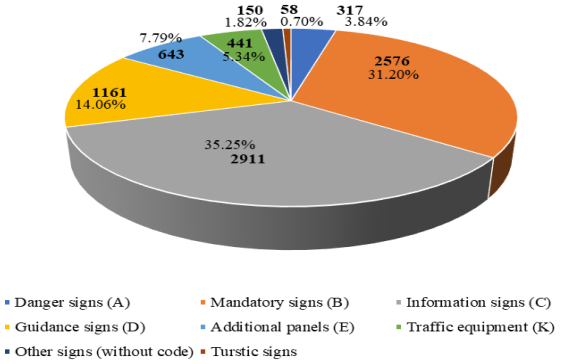


Fig. 9 *Total number of analyzed traffic signs classified by meaning on motorways*

The analysis of the retroreflective material from which traffic signs are made, showed that 7.59 % of all signs are made from Class I, 89.66 % from Class II and 2.75 % from Class III material (Figure 8). Croatian regulations for motorways demand only several signs to be made from Class III material, majority of the signs must be made from Class II. Although according to regulations, there should be no Class I signs on motorways, their share is relatively small (7.59 %).

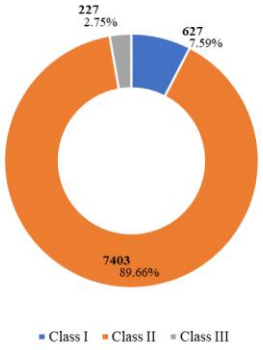


Fig. 10 *Total number of analyzed traffic signs classified by class of retroreflective material on motorways*

Regarding the age of traffic signs on Croatian motorways, average age of traffic signs is almost 11 years (Figure 11). Average age of traffic signs that are made from Class I is 9 years, Class II is 11 years and Class III 7 years.

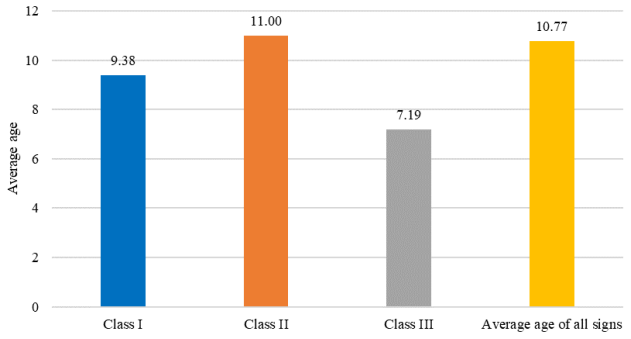


Fig. 11 *Average age of traffic signs by class of retroreflective material (years) on state roads*

Analysis of traffic signs according to the coefficient of retroreflection showed that the general condition of signs on motorways is satisfactory. 71.9 % of signs placed on the highway meet the minimum requirements of retroreflection and 28.11 % do not meet the minimum requirements of retroreflection. Of the total number of traffic signs, most traffic signs that meet the minimum requirements of retroreflection belong to traffic signs made of Class II. For traffic signs made of Class III, 2.31 % meet the minimum requirements while only 0.44 % do not meet the minimum retroreflection requirements (Figure 12).

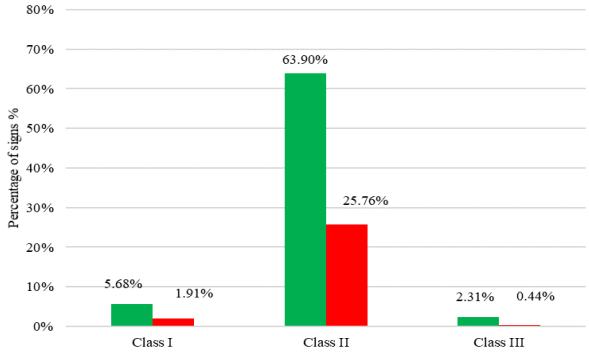


Fig. 12 *Total percentage of traffic signs by the class of retroreflective material that meet and do not meet minimum retroreflection values on state roads*

4. Conclusion

Traffic signalization is an integral part of every modern road and as such is a basic means of warning, regulating, guiding and informing traffic participants. The importance of traffic signals for the safety of the traffic system is especially evident in conditions of reduced visibility when drivers almost completely rely on traffic signals as the main source of information. Modern road traffic demands safe movement of users under normal circumstances and especially at night and/or in circumstances of reduced visibility. Quality solutions in the field of traffic signalization, especially traffic sings and road markings, can be achieved with relatively small investments and continuous maintenance.

In Croatia, retroreflection measurement of road markings and traffic signs are conducted by the Department for Traffic Signaling at the Faculty of Transport and Traffic Sciences for more than ten years. Methodology of measurement is based on the European and National standards and specifications. Benefits of this whole system are numerous. Some of them are, that this kind of system provides are reduction of maintenance cost, optimization of road maintenance activities, it provides up-to-date database, optimization of road maintenance patrol schedule, new information generated by maintenance patrol. System is useful in legal disputes, property protection and provides increase regarding of the road safety. Thus affects the safety of drivers, especially when driving in adverse weather conditions. Proof of this are the results of measuring the quality of road markings on state road as well as on motorways in Republic of Croatia. According to the presented results, it is visible that the level of retroreflection of road markings is continuously increasing during the measurement years. Several studies have shown a positive effect of quality maintenance of traffic signs and road markings on general road safety. The United Kingdom's Traffic Safety Foundation has issued a report on road safety monitoring on main roadways in 2013. The analysis has shown that traffic signs and road marking are one factor contributing to increased safety on seven out of ten analysed roads, leading to an 87 % reduction in overall number of injured. [12]

The collected results show that systematic road markings and traffic signs control plan can lead to the increase in their quality and thus results in more efficient maintenance system and improved visibility which ultimately leads to safer roads. In accordance with that, it is safe to say that constantly quality testing of road markings and traffic signs, can increase road safety. In addition, the lack of proper maintenance effectively cancels the safety benefits that can be gained through new vehicle technologies like ADAS systems, for instance Lane Departure Warning Systems (LDWS). Also, it is estimated that by 2025 at least half of the vehicles on Europe's roads will have some ability to "read" the road ahead. These vehicles will not work properly if the road markings and lines upon which they rely are not maintained to a high standard.

5. References

1. H. Fleyeh, J. Roch, 2013. *Benchmark evaluation of hog descriptors as features for classification of traffic signs*, International Journal for Traffic and Transport Engineering, 3(4): 448-464. doi: 10.7708/ijtte.2013.3(4).08

2. T. Miller, (1992). *Benefit-cost analysis of lane marking*, Transportation Research Record.

3. D. Babić, M. Fiolić, & D. Žilioniene, (2017). *Evolution of static and dynamic method for measuring retroreflection of road markings*. Građevinar

4. C. Debaillon and P. Carlson (TTI) Y. He, T. Schnell and F. Aktan (OPL), *Updates to Research on Recommended Minimum Levels for Pavement Marking Retroreflectivity to Meet Driver Night Visibility Needs*, Operator Performance Laboratory Center for Computer Aided Design the University of Iowa, (2007)

5. D. Babić, M. Modrić, D. Babić, M. Fiolić, (2019). *Evaluating the influence of road markings' retroreflectivity on road safety in low visibility conditions*, ZIRP, Zagreb

6. M. Ferko, A. Stažnik, M. Modrić, H Dijanić, (2019). *The impact of traffic signs quality of the frequency of traffic accidents*, Promet – Traffic & Transportation, Zagreb

7. P. Thurston: *Pavement Markings Role in Enhancing Road Safety Strategies*, Road marking Industry Association of Australia, (2009)

8. European, s. (n.d.). EN 1436 Materials for Road markings - Characteristics required for road users.

9. Guidelines and technical requirements for performing works on renewing road markings. Zagreb: Croatian Roads, (2010).

10. European, s. (n.d.). EN 12899-1: Fixed, vertical road traffic signs. In Part 1: Permanent signs.

11. Consiglio nazionale delle ricerche: Common understanding of assessment procedure (CUAP): Microprismatic retro-reflective sheetings, 2002.

12. European Union Road Federation. Improved Signage for Better Roads. An ERF Position Paper towards improving Traffic Signs in European Roads. Bruxelles; 2015. Available from: https://issuu.com/erf9/docs/erf_position_paper_on_vertical_sign

13. Ministry of the Sea, Transport, and Infrastructure, Available from: https://mmpi.gov.hr

The impact of COV - 19 pandemic on use of public transport in selected city in Slovakia

Daniela Šusteková[1], Lýdia Kontrová[2]
University of Žilina[1,2], Slovakia
Email:sustek@fpedas.uniza.sk, lydia.kontrova@fpedas.uniza.sk

Abstract: The aim of the article was to analyze the impact of lockdowns carried out during the Covid-19 pandemic in Slovakia in the years 2020 and 2021 on changes in public transport utilization in a selected locality. The sample city was the city of Košice in Slovakia and the sample contained data about the number of transported persons by public transport in this city during single days in the years 2018, 2019, 2020, 2021.

We created weekly time series from line graphs compiled for separate years. Subsequently, we analyzed the dynamics of individual time series using calculations of absolute and relative increments, basic indices, growth coefficients, absolute increment and total growth coefficient, and we modeled trends in time analysis and exponential adjustment for the observed years. We compared the years before the pandemic (2018, 2019) with the years most affected by the Corona crisis (2020, 2021). We evaluated the obtained data in the context of the timeline of ongoing lockdowns.

Key words: *LOCKDOWN, COVID - 19, TRANSPORT, Z - TEST FOR MEDIUM VALUE, TIME COUNCILS.*

1. Introduction

The Covid-19 pandemic has caused the worst economic and social shocks since the Great Depression in the 1930s. By the end of March 2022, Covid-19 had infected about 570 million people worldwide with more than 6.236 million deaths (Worldometer, April 22, 2022). Countries have had different approaches to resolve the crisis. Some have focused on economic stability and minimized Covid-19 restrictions, causing huge numbers of infections and deaths. In other countries, including Slovakia, governments have introduced locdowns to limit human contact and thus the spread of infection. The countries have suspended public transport, restricted entertainment establishments and banned public gatherings [1],[2].

Transport is one of the indicators for measuring sustainable development through overall energy consumption, transport growth, transport prices, and social and environmental impacts [3]. The challenge for many cities is to at least maintain the current number of passengers using public transport.

The Covid-19 pandemic has hit public transport hard in Slovakia as well. Number of passengers has dropped sharply and operators in several regions (especially in less developed towns) are currently facing difficult questions about their future viability. Several states of emergency and curfews have been declared in Slovakia, which have had a significant impact on the number of people using public transport. Even huge cities such as New York, Moscow, Milan and Paris, [4], did not escape from the sharp decline in population mobility between March 2020 and November 2020, as indicated by the data in Fig.1.

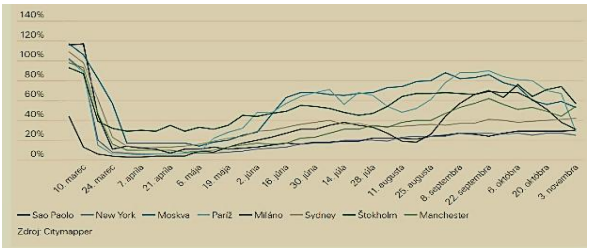


Fig1 1: *Decline in population mobility between March 2020 and November 2020 in selected cities*

The appropriate response from public transport operators to experienced events is to plan (anticipate) such unpredictable episodes in the future. A thorough analysis of the impact of the measures taken during the pandemic on changes in transport use is therefore appropriate.

The aim of the article was to analyze the impact of lockdowns carried out during the Covid-19 pandemic in Slovakia in 2020 and 2021 on changes in public transport utilization in a selected locality.

The chosen city was Košice and the sample contained data on the number of transported persons by public transport in this city on single days during the years 2018, 2019, 2020, 2021.

The obtained data were evaluated in the context of the timeline of ongoing lockdowns. We investigated how the closure of partial sectors (curfew, state of emergency, recommendation to work from home, closure of schools, services, restaurants, wellness, some workplaces, shopping centers, cultural institutions, sports grounds) affects the number of people transported in public transport and to what extent the use of public transport returned to its original numbers after the cancellation of individual lockdowns (whether the pandemic meant a global and permanent decline in the use of public transport or it was just a short-term phenomenon).

Based on the obtained data, we tried to answer the questions: Has the relationship of the population to the form of public transport changed? Has the confidence in this way of transport declined? If so, what are the main reasons, how can they be eliminated, what measures can be taken to stop this trend. We know that, given the negative effects on the environment, the increased orientation of the population towards car transport at the expense of limiting the use of public transport is not a welcome phenomenon.

2. Prerequisites and means for solving the problem

2.1. Creation of a timeline of persons movement in Slovakia in the years 2020 and 2021

In the first stage of the work, we created a timeline of states of emergencies, curfews and epidemiological measures announced in Slovakia in 2020 and 2021. Subsequently, we classified the time periods in terms of restrictions on movement to five levels:

1. Degree: mildest measures - obligation to wear respirators indoors, mandatory minimum distances, hand disinfection, relaxed measures and permitted visits to schools, shopping centers, churches, cultural and sport events, family celebrations, facilities providing various services.
2. Degree: moderate measures - obligation to wear respirators indoors, mandatory minimum distances, hand disinfection, open schools and school facilities, open shopping centers, churches, allowed cultural and sport events, facilities providing various services for a limited number of people.
3. Degree: stricter measures - obligation to wear respirators indoors, mandatory minimum distances, hand disinfection, closed schools and school facilities, ban on DSS and hospital visits, open churches with limited number of persons, acceptable cultural and family events for a small number of people, facilities providing various services for only a small number of people.

4. Degree: strict measures - declared state of emergency, closure of schools, shopping centers, service operations, limited time of free movement and gathering of persons.
5. Degree: the strictest measures - state of emergency and curfew, citizens only allowed to go to work, medical facilities and to purchase basic needs.

After getting acquainted with the decrees (directives) concerning pandemic measures, which were published by the Government of the Slovak Republic in 2020 and 2021, we created relevant tables and subsequently graphs of restrictions on the movement of persons.

When creating graphs, we applied the time variable (week) to the horizontal axis and to the vertical axis the degree of the restriction according to the valid directive, which was valid in the given period.

We obtained bar graphs - Graph 2, Graph 3. These data were then used to evaluate the correlation between the number of public transport passengers and the degree of restriction of movement in the analyzed weeks.

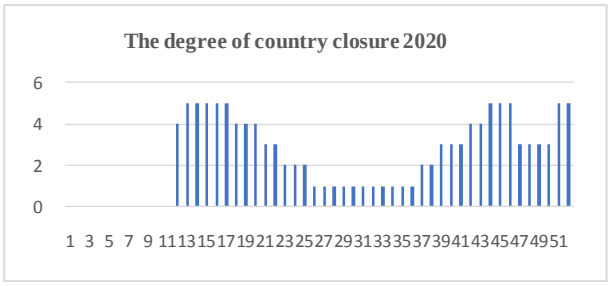


Fig. 2 *The degrees of country closure 2020*

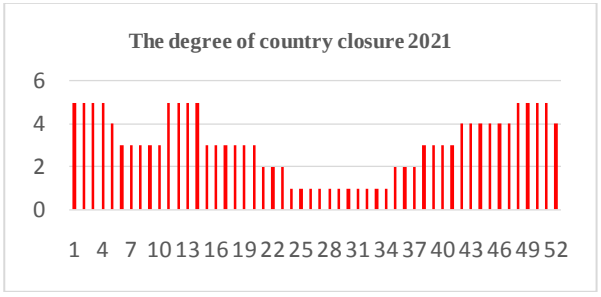


Fig. 3 *The degrees of country closure 2021*

In Slovakia during 2020, according to our classification, there was a degree of threat of either 4 or 5 (maximum restriction of movement of persons) from March 15 to May 20. Subsequently, in the autumn, with the onset of the second wave of the pandemic, there was the closure of service operations and restrictions on the movement of persons according to level 4 or 5 from October 1, 2020 to November 16, 2020. As of December 19, the curfew and the strictest level of restrictions on the movement of persons were announced. These lasted with a short release until the end of March 2021. Since mid-April, the situation with the number of people infected with the coronavirus has gradually improved. In the summer of 2021, measures and the movement of persons were relaxed, but they were bound to a confirmation about a vaccination or a negative coronavirus test.

2.2. Statistical analysis of the dates

We created a weekly time series from the daily data of the number of passengers obtained from the transport company of the city of Košice. We obtained initial information for the analysis of these time series from line graphs compiled for separate years. We applied the time variable (weeks) on the horizontal axis and the time series values (number of public transport passengers) on the vertical axis. We plotted the values of four time series in a line graph. Graphs of the annual values of the weekly time series of the number of public transport passengers in Košice in the period 2018 - 2021 show how the level of values in the given seasons differs during the entire time series. (Fig. 4)

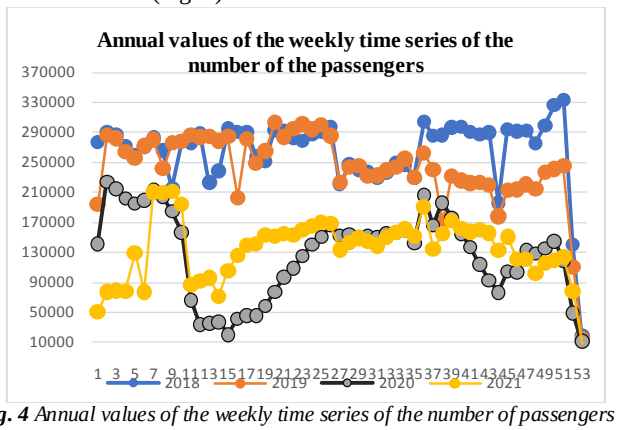


Fig. 4 *Annual values of the weekly time series of the number of passengers*

3. Solution of the examined problem

The course of the graphs in 2018 and 2019 led us to the idea of comparing the numbers of passengers per week in public transport in Košice in these periods. We wanted to confirm the hypothesis of equal occupancy of public transport in Košice in 2018 and 2019, i.e. to confirm the assumption that in the years before the pandemic, the weekly number of public transport passengers in Košice was approximately at the same level.

We used a two - tailed z - test for the mean, given that the ranges of both random samples were large enough, n> 30 [5].

We tested the hypothesis

$H_0: \mu_1 = \mu_2$ against $H_1: \mu_1 \neq \mu_2$.

We chosen the commonly used $\alpha = 0{,}05$.

The output from Excel (Table 1) indicates the P-value at the level $P = 0{,}49$.

The test at the 5% level of significance proved that we do not reject the null hypothesis: the occupancy of public transport in the city of Košice in 2018 and 2019 was at approximately the same level, i.e. the weekly numbers of transported passengers in these years were approximately the same.

Table 1: ***z****-Test: Two Sample for Means*

z-Test: Two Sample for Means		
	Variable 1	*Variable 2*
Mean	265568,3396	244103,3396
Known Variance	2,65562E+14	2443405562
Observations	53	53
Hypothesized Mean Difference	0	
z	0,009589227	
P(Z<=z) one-tail	**0,49617451**	
z Critical one-tail	1,644853627	
P(Z<=z) two-tail	0,992349021	
z Critical two-tail	1,959963985	

Subsequently, we performed a simple exponential compensation with the selected compensation constant α = 0.7 to determine the trend of non-seasonal swaying time series. We obtained "smoother curves", the course of which we compared to the graphs of movement restrictions (Fig. 5).

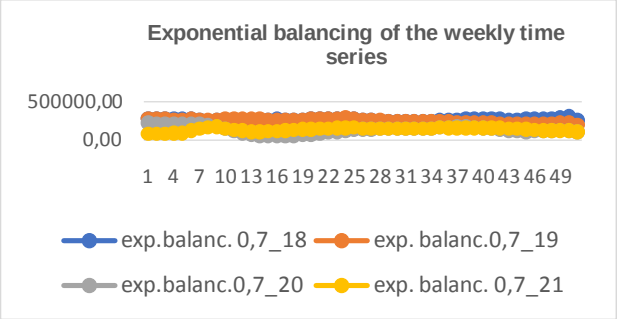


Fig. 5 *Exponential balancing of the weekly time series*

The analysis of the obtained graphs brought these conclusions

- As we can see from the graphs, the number of people using public transport in the city of Košice is declining from year to year. The reason is obviously the fact that more and more people prefer a more comfortable way of transport by their own car. The number of people who can afford this mode of transport is also growing.
- In 2018 and 2019, we registered very similar numbers of transported persons in individual weeks of the year. Interesting is the almost identical occupancy of public transport during the summer holidays in both years.
- We recorded the largest decrease in the number of transported persons during the announcement of the first curfew in Slovakia in March 2020. In this period, the inhabitants very strictly adhered to the government's regulations and "life in Slovakia" really almost stopped.
- The year 2021 no longer brought such a remarkable decrease in the mobility of citizens, as a large number of measures were targeted at unvaccinated persons, while vaccinated persons had a greater degree of freedom of movement. Here again, we register an interesting match in the number of transported persons in 2020 and 2021 during the summer holidays.

In the next stage of the work, we calculated the dynamics of the obtained time series.

Simple measures of time series dynamics allowed us to accurately characterize the basic features of the "behavior" of the time series, determine the periods of greatest growth (decrease) in the number of passengers, or the average weekly percentage decrease of passengers in the analyzed seasons.

We evaluated the dynamics of time series using calculations of absolute and relative increments of the series (delta1, delta2) and basic indices. We determined the acceleration or deceleration of the trend on the basis of calculations of chain indices, growth coefficients, and average growth coefficient [6].

Data tables compiled in MS Excel (Table2, Table3) were crucial for us.

We derived the answers to the questions we asked above mainly from the sixth column in the Table 2 iR = ki (see pink), which reflects the average weekly percentage decrease (or increase) in the number of passengers.

After finding the maximum and minimum value of the chain indices iR = Ki in the sixth column of Table 2, we obtained information on where, when and how the number of public transport passengers changed the most.

As an example, we present a part of the table of time series data for the year 2020 (Table 2).

We summarize in Table 3 the important information about the given years, such as the average number of passengers, the maximum, the minimum, the average weekly growth (decrease) of passengers, the average weekly slowdown in the number of passengers and the average weekly percentage decrease in the number of passengers.

Table 2: *Time series data for 2020*

week	*2020*	*delta 1 i*	*delta 2 i*	*iB*	*iR=k i*	*Ti*	*Ti*
1	223000	X	X	1	X	X	X
2	223688	688	X	1,003085	1,00	100,31%	0,31%
3	214772	-8916	-9604	0,963103	0,96	96,01%	-3,99%
4	201609	-13163	-4247	0,904076	0,94	93,87%	-6,13%
5	**195009**	-6600	6563	0,87448	0,97	96,73%	-3,27%
6	**199399**	4390	10990	0,894166	1,02	102,25%	2,25%
7	**213309**	13910	9520	0,956543	1,07	106,98%	6,98%
8	**203394**	-9915	-3825	0,912081	0,95	95,35%	-4,65%
9	**184775**	-18619	-8704	0,828587	0,91	90,85%	-9,15%
10	**156595**	-28180	-9561	0,70222	0,85	84,75%	-15,25%
11	**66476**	-90119	-1939	0,298099	0,42	42,45%	-57,55%
12	**33441**	-33035	57084	0,14996	0,50	50,31%	-49,69%
13	**35509**	2068	35103	0,159233	1,06	106,18%	6,18%
14	**37391**	1882	-186	0,167673	1,05	105,30%	5,30%
15	**20198**	-17193	-9075	0,090574	0,54	54,02%	-45,98%
16	**41248**	21050	38243	0,184969	2,04	204,22%	104,22%
17	**45551**	4303	-6747	0,204265	1,10	110,43%	10,43%
18	**45602**	51	-4252	0,204493	1,00	100,11%	0,11%
19	**58102**	12500	12449	0,260547	1,27	127,41%	27,41%
20	**76914**	18812	6312	0,344906	1,32	132,38%	32,38%
21	**96985**	20071	1259	0,43491	1,26	126,10%	26,10%

Table 3: *Data related to transported persons*

year	2018	2019	2020	2021
average	265821	245721	129919	135225
maximum	333182	303163	223688	211051
minimum	196684	15008	11246	8914
Delta1	-5211	-5096	-4072	-1290
Delta2	-2368	-1994	-762	-1399
Average iR =Ki	0,949	0,945	0,949	0,95

4. Results and Discussion

The lowest weekly percentage decrease in 2018 in the time series occurred in week 52 (to 42%) and week 53 (to 14%). The highest percentage increase was in week 45 (149%).

The lowest weekly percentage decrease in 2019 in the time series occurred again in week 52 (to 45%) and week 53 (to 13%). The highest percentage increase was in week 17 (139%).

The lowest weekly percentage decrease in 2020 in the time series occurred in weeks 11 (to 42%) and weeks 53 (to 22%). Both periods correspond to the periods of introduction of the strictest restrictions on the movement of persons. We recorded the highest percentage increase in week 16 (204%), which was at the time of the release of the government measures.

The lowest weekly percentage decrease in 2021 in the time series occurred in week 52 (to 11%). We recorded the highest percentage increase in week 7 (270%), which was at the time of the release of the government measures.

The obtained results also point to the fact that the number of public transport passengers has decreased significantly not only in Slovakia and there may be several reasons:

- ✔ People avoid public transport because they anticipate the risk of infection, which has not yet been confirmed by any relevant research. A study in Paris declared that none of the 150 epicenters of the coronavirus infection came from the city's transport systems. A similar study in Austria declared that none of the 355 cases infected with the coronavirus in April and May 2021 were traced to public transport[7].
- ✔ If transit itself was a super-spread spot, then a large outbreak would be expected, for example, in Hong Kong (7.5 mil. population) dependent on public transport, which transported about 12.5 million people a day before the pandemic[8]. According to the study, the number of passengers there has decreased less than in other systems in the world, and yet they have recorded only about 1,100 cases of infection. Replacement of public transport with individual (car) transport is unbearable. Nowadays, more than 1.3 million people die every year of road accidents and another 4.2 million die of the health effects of air pollution[9].

5. Conclusion

The world after COVID-19 is facing unprecedented challenges. Nevertheless, this global pandemic presents opportunities to raise cities and countries' awareness of their transport needs and infrastructure, and in some cases to reduce transport dependence and move towards more resilient and sustainable transport infrastructure and operations in the future. Public transport, despite the potential for reducing social distance, is nevertheless the only possibility of transport available to many people.

The challenge for many cities is to at least maintain the current number of passengers using public transport[11] and [12] identified in their research several factors by which providers and passengers can, to some extent, influence the demand for public transport.

Through the public transport policy of individual cities, regions, and states, stabilization of the demand for public passenger transport (PPT) is achievable [13],[14]. The relationship between satisfaction with PPT and way of transport has been investigated by Diana [15], Cantwell et al.[8] and Abouhassan [9].

The governments of all the concerned countries face the following challenges:

- ✔ They must protect the survival and efficiency of public transport while ensuring safe mobility during a pandemic (unforeseen events).
- ✔ Without proper investment in public transport accessibility, the developing middle class will focus more on individual transport, which will jeopardize the sustainability of public transport.
- ✔ Reducing public transport availability can likely lead to higher unemployment, weakened access to labor market opportunities and damage the city's productivity.
- ✔ For many less developed cities, it is the right time to take the opportunity to think about reorienting the public transport network and securing a more reliable network, as well as increasing coverage.
- ✔ After overcoming the pandemic, people will choose services that offer better reliability, lower costs, convenience, safety and sustainability. Public transport must be prepared to capture this return to market.
- ✔ Decisions for public transport on an emotional and economic level.
- ✔ The coming years will be crucial in showing how many people will work from home or use individual transport.
- ✔ Public transport is rarely profitable, but it is essential for the success of large cities - a reduction in public transport costs can be compared to "killing a hen that lays golden eggs".
- ✔ Revitalized transportation systems do not need hospital-level disinfection to function safely. What can help is to expand contactless payments, a new culture of transit, hand washing at bus stops (practiced in Korea).
- ✔ According to the results in terms of reducing traffic in the Underground compared to transit "above" the ground, it has been shown that passengers feel more threatened by travelling "underground".
- ✔ Anticipating the number of passengers and providing real-time response so as to avoid crowding; implementing contactless payment systems; and providing regular and transparent communications to staff and passengers [17].

Coming out of the pandemic, it is essential that governments learn to use these resources to make evidence-based decisions about infrastructure and investments to make the very best transportation systems for their countries and cities.

The road out of the pandemic runs along tram rails, demarcated lanes for buses and trolleybuses.

Acknowledgement

This publication was created thanks to support under the Operational Program Integrated Infrastructure for the project: *Identification and possibilities of implementation of new technological measures in transport to achieve safe mobility during a pandemic caused by COVID-19* (ITMS code: 313011AUX5), co-financed by the European Regional Development Fund.

6. References

1. R. M. Anderson, H. Heesterbeek, D. Klinkenberg, T. D. Hollingsworth, *How will country-based mitigation measures influencethe course of the COVID-19 epidemic*, ?Lancet,395, 931–934. (2020)

2. J.A. Lewnard, Lo, N.C. *Scientific and ethical basis for social-distancing interventions against COVID-19*, Lancet Infect. Dis.,20, 631–633. (2020)

3. A. Kalašová, V. Harantová, K.Culík, *Public transport as a part of shared economy.*Arch. Automot. Eng. Arch. Motoryz.,85,49–56. (2019)

4. J. Sung, Y. Monschauer, *Covid-19 is changing our behaviour and transport energy use patterns*, Changes in transport behaviour during the Covid-19 crisis, 27 May (2020), https://www.iea.org/articles/changes-in-transport-behaviour-during-the-covid-19-crisis?msclkid=89100f35c62911ec86c640646fd69e74

5. A.Tirpáková, *Štatistické metódy a ich aplikácie*, FPV UKF Nitra (2011)

6. M. Sebera, *Časové rady*, Masarykova univerzita Brno, FSS (2014)

7. *Here's how to build better public transport after COVID-19,* 30 April, World economic forum, (2021), www.weforum.org/agenda/2021/04/how-improve-public-transport-after-covid- 19/?msclkid=890f2ae6c62911ec9ed21e42438905ac

8. J. Sadik-Khan, S. Solomonow, *Fear of Transit Is Bad for Cities - The Atlantic*, June 14, (2020) https://www.theatlantic.com/ideas/archive/2020/06/fear-transit-bad-cities/612979/

9. J.Bird, S. Criticis, N. Tsivanidis, *Impact of COVID-19 on public transport*, The International Growth Centre, 6 Aug, (2020), https://www.theigc.org/blog/impact-of-covid-19-on-public-transport/

10. C. Polat, *The demand determinants for urban public transport service*, A rewiev of the literature J. Appl. Sci.,12, 1211–1231, (2012)

11. N. Paulley, R. Balcome, R. Mackett, H. Titheridge, J. Preston, M. Wardman, J. Shires, P. White, *The demand for publictransport: The effects of fares, quality of services, income and car ownership*,Transp. Policy, ,13, 295–306, (*2006)*

12. D. Metz, *Demographic determinants of daily travel demand.*, Transp. *Policy*,21, 20–25, (*2012)*

13. G. Currie, *Exploring links between the sustainability performance of urban public transport and land use in international cities*., J.Transp. Land,11, 325–342, (2018)
14. J. Holmgren, *A strategy for increased public transport usage—The effects of implementing a welfare maximizing policy*., Res.Transp. Econ., ,48, 221–226 (2014)
15. M. Diana, *Measuring the satisfaction of multimodal travelers for local transit services in different urban contexts*, Transp. Res.Part A Policy Pract.,46, 1–1, (2012)
16. M. Cantwell, B. Caulfield, M. O´Mahony, *Examining the factors that impact public transport commuting satisfaction*. J. PublicTransp.,12, 1–21, (2009)
17.M. Abouhassan, *Urban transport systems analysis*, Wit Trans. Built Environ.,176, 57–68. (2017)
18. *Can public transportation survive the pandemic? Experts warn of 'death spiral' (nbcnews.com)*, Decembre, (2020) https://www.nbcnews.com/tech/tech-news/can-public-transportation-survive-pandemic-experts-warn-death-spiral-n1252214

Development of an 1D simulation model to optimize performance and emissions of large gas engines

Dimitar Dimitrov[1], Gernot Kammel[1], Erich Egert[1], Nicole Wermuth[1], Andreas Wimmer[1,2]
LEC GmbH (Large Engines Competence Center), Graz, Austria [1]
Graz University of Technology, Graz, Austria [2]

Dimitar.Dimitrov@lec.tugraz.at

Abstract: *The main subject of this paper is the development of a multicylinder engine model for the prediction and optimization of engine performance based on one-dimensional (1D) simulation. 1D simulation is widely used to preoptimize engine geometry and operating parameters to achieve performance targets and comply with operational and emission constraints. Due to the short calculation times, 1D simulation allows the evaluation of a larger number of variants. As new engine concepts are developed, many operating parameters are first defined and optimized with a 1D multicylinder engine model. This model illustrates the full complexity of the engine with its geometry, turbocharging and combustion parameters. In this paper the design of experiments (DoE) method is used in connection with 1D simulation to determine the optimal engine configuration as well as parameters related to the combustion process, i.e., valve timing, compression ratio, ignition timing, excess air ratio. This approach enables the determination of the maximum engine efficiency while taking the boundary conditions and the constraints of nitrogen oxide emissions (NOx) and knock into account. The method also enables the reduction of the cylinder-to-cylinder deviations by improving the gas dynamics and the fuel metering in the main combustion chamber and in the pre-chamber, which is especially important for the multicylinder engine. The simulation results are validated with experimental investigations on a single cylinder research engine.*

Keywords*: GAS FUELED ENGINES, 1D SIMULATION*

1. Introduction

In recent years the demand for high-performance engines has increased, which drives their continued development. When a new gas engine is being developed, a global optimum for the operating parameters should be found so that the engine can be operated at the best possible efficiency and the required power output without the occurrence of knock and while complying with valid emission legislation. Whereas the current German legislation [1] for gas engines defines the nitrogen oxide emissions limit as 500 mg/m³ (norm) @ 5% O2, the trend is towards a further reduction to 250 mg/m³ (norm) @ 5% O2 (Gothenburg Protocol [2]) or 75 mg/m³ (norm) @ 15% O2 (EU Directive 2010/75/EU [3]). This paper describes the evolution and the important role of 1D simulation modeling in the development of a new high-performance gas engine. The required sub-models and boundary conditions are discussed and an application is provided as an example of successful use of the methodology.

2. LEC Development Methodology

The 1D simulation that is part of **LDM** (**L**EC **D**evelopment **M**ethodology) [4] is an efficient tool that meets the demands for flexibility, predictability and computational time for this type of investigations. LDM is based on the intensive interaction between simulation and experimental investigations on single cylinder research engines (SCE) and multicylinder engines (MCE), see Figure 1. This methodology makes use of 3D CFD simulation and 0D/1D engine cycle simulation. While 3D CFD simulation is mainly employed to optimize the details of relevant processes (e.g., mixture formation and combustion in the prechamber and main combustion chamber, determination of the location of knock), 0D/1D engine cycle simulation is applied to pre-optimize significant engine parameters (e.g., compression ratio, valve timing). When applying the LDM methodology, it must be guaranteed that the results from single cylinder tests can be transferred to the multicylinder engine. For this it is necessary to acquire boundary conditions at the SCE to get conditions comparable to the ones of the multicylinder engine. Not only the thermal boundary conditions but also the conditions at the beginning of the intake stroke (temperature, pressure, and in-cylinder gas composition) are required. These conditions are determined in an iterative process based on 1D engine cycle simulation of the multicylinder engine and the single cylinder setup. The design of the single cylinder test bed has some specific features. While the piping system of the single cylinder engine test bed is being designed, it is important to adapt the gas dynamics in the intake and exhaust piping system. The objective is to achieve similar conditions in the cylinder of the SCE and the corresponding multicylinder engine.

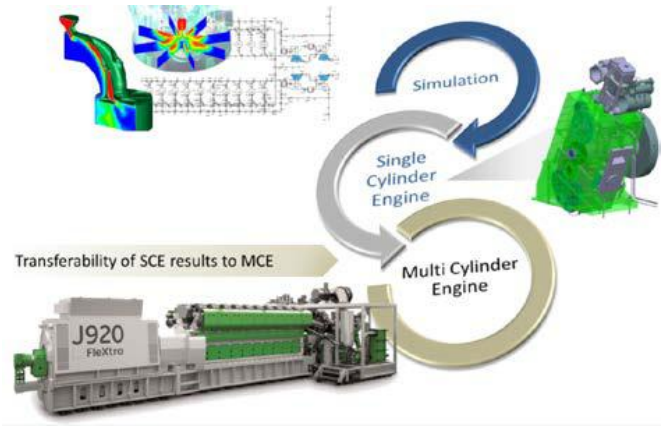


Fig. 1 *LDM: LEC Development Methodology*

3. Database and data analysis for the calibration and verification of the 1D model

For following the LDM, in a first step a reference case has to be created using measurement data from a physical engine with the purpose of further development and calibration of the simulation model. The SCE configuration, described in this paper, is equipped with gas scavenged pre-chambers and about 6 dm³ cylinder displacement volume. The available database includes measurements for variations of compression ratio, NOx emission level, ignition timing, intake charge temperature, pre-chamber energy and exhaust gas pressure. Configurations with two different valve lift profiles were used. Furthermore, measurement some performed at the knock limit.

Measurement data are required for the development and calibration of models as well as for the calculation of the rates of heat release for direct specification in the 1D simulation. Developed at the LEC, the engine cycle calculation program LEC CORA is used to analyze the operating points measured on the test bed. The software package CORA (Combustion Optimization, Research and Analysis) was designed to analyze and simulate the high-pressure cycle of the working process of combustion engines. It enables the

analysis of measured pressure traces as well as simulation of cylinder conditions during the high-pressure cycle upon specification of the rate of heat release histories or the rate of heat release models. The software is used in combustion analysis mainly for pressure offset, compression ratio and top dead center adjustment as well as pressure history analysis (high-pressure cycle) and loss analysis.

The high demand on the quality of the measurements used as a basis for analysis, leads to the necessity to check this quality, whenever possible directly and automatically at the test bed, to allow early detection of errors [5]. In this context, a methodology for automated error diagnosis on engine test beds was developed at the LEC. The algorithms this system is relying on, are provided in the "LEC MCheck" (LEC Measurement Check System) software solution and are used directly on the test bed. A consistent use of these tools guarantees a high quality of measurement data and the resulting rate of heat release histories, which in turn is advantageous, when calibrating simulation models and interpreting the results.

4. Development of the MCE model

As baseline simulation model, the MCE model with pre-chambers for each cylinder, gas mixers and two stage turbocharging, is used. The compressors and turbines are depicted with corresponding maps. The model is created using the commercial software package GT Power. One challenge in the development of a pre-chamber gas engine simulation model is to determine the conditions, not only in the cylinder, but also in the pre-chamber (PC) as accurately as possible, because the combustion in the PC influences the behavior of the main chamber. For this reason, also the pre-chamber, pre-chamber gas valve and the piping system of the PC gas rail are depicted in the 1D model for each cylinder. The pre-chamber gas valve is a check valve, and it is modelled with high complexity: pin mass, valve spring stiffness, valve maximum displacement and flow coefficients. The pre-chamber gas rail is also modelled in detail, in order to reproduce the gas dynamics in the rail and the fuel flow into the pre-chamber thoroughly.

4.1. Modelling of the combustion process

1D simulation requires the rate of heat release in the cylinder and in the PC. Measurement data from relevant operating points, measured on SCE, are used to determine the actual rate of heat release history using engine cycle calculation. The combustion duration in the cylinder and the fraction of fuel burned are additionally adjusted as functions of excess air ratio (EAR), because those parameters are strongly dependent on EAR. Those functions are determined from measured EAR variations on the SCE test bed, Figure 2.

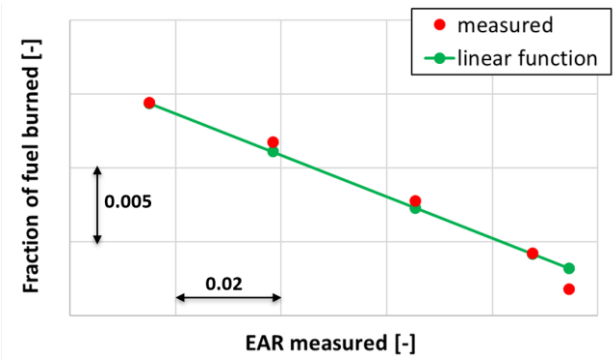


Fig. 2 *SCE measurement: Fraction of fuel burned as a function of EAR.*

Figure 3 represents the implementation of the functions for combustion duration and fraction of fuel burned in the cylinder module of the 1D MCE model.

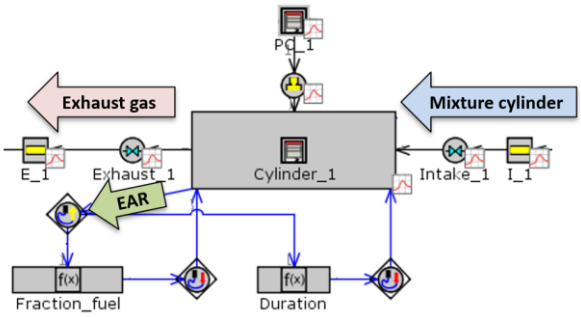


Fig. 3 *Implementation of the functions in the MCE model*

4.2. NOx model and knock prediction

The NOx concentration that arises during combustion is calculated from the well-known Pattas and Häfner model [6] in the used software, which accounts for the formation of thermal NO using an extended Zeldovich mechanism. The temperature of the burned zone for simulating the post-flame reactions is calculated from the heat release rate (ROHR) model with a two-zone sub-model. In addition, the two-zone modeling approach enables to determine the maximum temperature in the unburned combustion zone, which is assumed as a reasonable indicator of conditions for knock events and as a criterion for the knock limit. The assumption is, that the knock behavior of the engine stays unchanged in case that this temperature is constant. Another possibility for knock prediction is the application of the LEC knock model [7]. The basic idea behind this model is to ascribe the statistical phenomenon of the occurrence of knock-cycles to the similar statistical phenomenon of the ignition delay scatter. The method uses models for the ROHR, knock timing and knock intensity. Because the LEC knock model requires a wide measurement database with operating points at the knock limit for its calibration, typically it is not used at this stage of the engine development.

4.3. Other features of the MCE model

In most of the common applications, large-bore gas engines operate at constant NOx emission levels. For this reason, a NOx-controller is implemented in the MCE model, so that it continuously varies the EAR until the target NOx level is reached.

One issue, when using such a highly complex model, is the relatively long computing time. In order to reduce it, for some investigations the turbochargers are replaced with a block, which uses a function for calculation of the exhaust back pressure. The function is based on the turbocharger main equation [8], and in this case it is possible to use a constant turbocharger efficiency and constant compressor bypass ratio. For the adjustment of the exhaust back pressure in the model an orifice connection in the exhaust piping of the model is used.

With respect to NOx-emission, the 1D MCE model typically is calibrated by using NOx variations measured on a single cylinder research engine. With this approach very good agreement of the simulation results with the measured EAR at the same NOx level can be achieved. Due to the high complexity of the system and the large number of free parameters, the statistical method Design of Experiment (DoE) is a useful tool to support this calibration. The free parameters optimized on the basis of this approach are typically compression ratio, control of the combustion process, valve timing and turbocharger design. The typical goal of the investigations is to achieve the highest engine efficiency possible while fulfilling the boundary conditions of permissible NOx emission limits, maximum cylinder peak firing pressure and knock-free operation [9]. Figure 4 provides an overview of the optimization process using the DoE method.

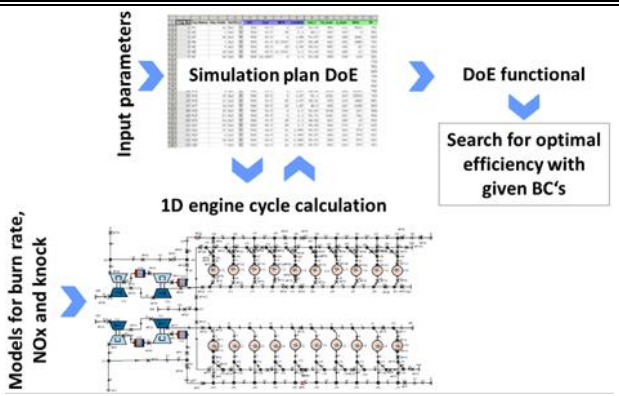


Fig. 4 *Procedure for applying DoE methods for 1D simulation.*

5. Applications of the 1D simulation model and results

Different engine configurations were compared with the 1D MCE model. First, the model was calibrated on the base of SCE measurements. Thereby different measurement series were used: Brake mean effective pressure (BMEP) variations, NOx variations, as well as measurements at the knock limit. The following configurations were investigated:

- base concept with Miller valve timing, compressor bypass and mixture preparation with a gas mixer,
- mixture preparation with port fuel injection (PFI) for each cylinder instead of a centrally located gas mixer for all cylinders and control of the peak firing pressure,
- mixture preparation with gas mixer and variable valve control.

The simulations with the 1D model have shown that all configurations have similar EAR deviations from the average value in the PC at ignition timing. In order to balance those EAR deviations in the pre-chambers, PC solenoid valves can be used instead of check valves.

The implementation of the PFI for each cylinder instead of a gas mixer is a potential improvement. In the case of PFI, a gas valve admits the fuel into the intake port in front of the intake valve, then the mixture of air and fuel flows into the cylinder, when the intake valve is open. The objective is a reduction of the cylinder-to-cylinder deviations of the multicylinder engine, because the PFI concept allows a cylinder-specific fuel control. As a consequence, the balancing of the peak firing pressure is possible.

The application of variable valve control, allows a zero compressor bypass and as a consequence an efficiency increase and a reduction of unburned hydrocarbon emissions (HC), but it also requires more procurement costs and leads to higher friction losses.

There is high potential in the layout of the valve lift curves for the first two configurations above. The valve lift curves influence the cylinder temperature, residual gas content and as a consequence the nitric oxide emissions formation and the knock tendency. In addition, the valve overlap is responsible for a part of the HC emissions.

With the defined BMEP and NOx-level as target values a high-end gas engine is optimized using the 1D MCE model. Thereby the design of experiments method is used. The target is to increase the engine efficiency, on the condition that NOx and peak firing pressure must not exceed the previously given values. Following factors for the DoE investigation are chosen: position of the ROHR (crank angle at 50% mass fuel burned in the cylinder, MFB_50%), intake valve opening, intake valve closing, exhaust valve opening and exhaust valve closing. The constraints are knocking combustion (described by the maximum temperature in the unburned zone) and EAR. Measurements on the SCE test bed have shown that the combustion stability deteriorates once the EAR exceeds a critical threshold. With the help of the commercial software MODDE a simulation plan with 26 cases is generated, the cases are simulated, and mathematical models for prediction of engine efficiency, temperature of the unburned zone and peak firing pressure are created. Figure 5 shows the very good agreement between the observed values and the predicted ones. With the help of the optimizer tool in the MODDE software the optimal variant is determined, and the valve timings for a new camshaft can be fixed. With the newly designed and machined camshaft measurements on the SCE test bed with variation of ignition timing and compression ratio have been performed.

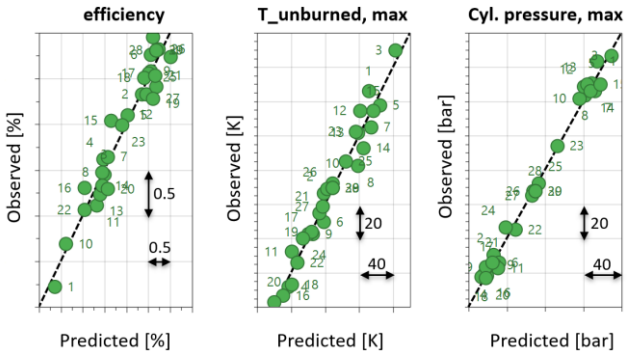


Fig. 5 *DoE investigation: observed vs. predicted values.*

The measurements have confirmed the optimal MFB_50% for maximal engine efficiency from DoE investigation. The efficiency gained by the compression ratio increase from simulation and from measurement are also in the same range. The measurements confirmed also the efficiency increase with the new valve lift profile.

6. Summary and outlook

This paper presents the relevance of 1D simulation during the development process of high-performance large bore gas engines by taking different development constraints into account. 1D simulation models of different designs and at different levels of detail were discussed in relation to each specific issue. The model was calibrated on the base of SCE measurements. As a result, it was possible to increase the BMEP and engine efficiency. The simulation results were confirmed by measurements at the SCE test bed.

Further investigations are planned with increased compression ratio and adaption of the MFB_50%.

7. References

[1] German Federal Government, 44. BImSchV - Vierundvierzigste Verordnung zur Durchführung des Bundes Immissionsschutzgesetzes* (Verordnung über mittelgroße Feuerungs- Gasturbinen- und Verbrennungsmotoranlagen - 44. BImSchV), 2019. https://www.gesetze-iminternet.de/bimschv_44/BJNR080410019.html (accessed June 16, 2021)

[2] Gothenburg Protocol "Protocol to the 1979 convention on long-range transboundary air pollution to abate acidification, eutrophication and ground-level ozone". Gothenburg 1999, online: http://www.unece.org/env/lrtap/multi_h1.html

[3] European Parliament and Council "Directive 2010/75/EU of the European Parliament and of the Council of 24 November 2010 on industrial emissions". In: Official Journal of the European Union, vol. 53, 2010, No. L33

[4] Sauperl, I., Wimmer, A., Dimitrov, D., Zelenka, J., Pirker, G., Schneßl, E., Winter, H.: Ldm compact - a methodology for development of gas engines for use with low environmental impact non-natural gas, Strojniški Vestnik - Journal of Mechanical Engineering. 64, 12, p. 743-752, 2018

[5] Wohlthan, M., Pirker, G., Krenn, M., Wimmer, A.: LEC-MCheck – Eine Methodik zur Fehlerdiagnose an Motorprüfständen. 15th Conference „The Working Process of the Internal Combustion Engine“, 2015

[6] Pattas, K.; Häfner, G.: Stickoxidbildung bei der ottomotorischen Verbrennung, Motortechnische Zeitschrift, MTZ 34 (1973), 12

[7] Dimitrov, D., Chmela, F., Wimmer, A. (2005). Eine Methode zur Vorausberechnung des Klopfverhaltens von Gas-motoren. 4. Dessauer Gasmotoren Konferenz. (in German)

[8] Merker, G. P., Schwarz, Ch. (Hrsg.): "Grundlagen Verbrennungsmotoren", 2009, pp. 353-354.

[9] Krenn, M., Pirker, G., Mühlberger, M., Wimmer, A.: Einsatz der DoE-Methode zur simulationsbasierten Optimierung von Großgasmotoren. 14. Tagung Der Arbeitsprozess des Verbrennungsmotors, Graz, 2013.

8. Acknowledgments

The authors would like to acknowledge the financial support of the ‘‘COMET - Competence Centres for Excellent Technologies’’ Programme of the Austrian Federal Ministry for Transport, Innovation and Technology (BMVIT), Austria, the Austrian Federal Ministry for Digital and Economic Affairs (BMDW), Austria and the Provinces of Styria, Tyrol and Vienna for the K1-Centre LEC EvoLET. The COMET Programme is managed by the Austrian Research Promotion Agency (FFG).

Methane number influence on the dual fuel four stroke marine engine performance at high load range

Delyan Hristov
Nikola Vaptsarov naval Academy Varna, Bulgaria
d.hristov@nvna.eu[1], d.hristov@naval-acad.bg[1]

Abstract: *In the present publication it is considered the technology and the features of the operation of the newly introduced in the marine industry wide spreading dual fuel four stroke engines. There are analysed the significant differences between the conventional Diesel engines and the dual fuel Otto engines in their operation process. The influence of the gas fuel quality in the case of the dual fuel engines is in the main concern underlined. Simulation based experiment is carried out for data attaining, related to the performance of the dual fuel engines influenced by the fuel quality on high load range. The acquired data is analysed, and evaluation of the engine derating outcome is performed. On the base of the results are stated conclusions and recommendations to be followed by the engineering crew members dealing with such kind of engines on board LNG fuelled ships.*
Keywords*: LNG METHANE NUMBER, OTTO CYCLE MARINE ENGINE, KNOCKING OF THE ENGINE, GAS FUEL QUALITY, HIGH LOAD OPERATION*

1. Introduction

In the transition time of shipping decarbonization the intermediate way to partly reduce the carbon emissions is the use the LNG as fuel. Although there are different approaches to improve the efficiency and to reduce the emissions from ships [1, 2, 4, 5, 13], there is no such fuel available fuel nowadays as the natural gas to be able in due time to cover the infrastructure and technological demand in same time with such reduction of the harmful engine emissions.

Aside from the safe issues with the handling and storage of the LNG onboard there are other technical challenges in the operation of the dual fuel engines with their specific features compared to the conventional marine diesel engines.

Most of the electrical generator driving engines operating on LNG rely on the dual fuel Otto cycle concept. Special feature of this type of engines is that they have to keep proper air/fuel ratio in a specific narrow range, so to achieve low emission operation as they are intended as a main difference with the Diesel cycle engines.

With the special features of the dual fuel four stroke engines most of the marine engineers are not aware of. In this publication the aim is to represent the influence of the LNG quality to the engine normal operation. Especially the influence of the methane number to the ability the engine to be loaded to specific range without safety issues. The tasks scheduled to be performed are:

- To clarify the four-stroke dual fuel Otto cycle engines features
- To perform experiment in a simulated environment with four stroke dual fuel engine with different grades natural gas, so to express the influence of the fuel quality to the combustion process.

2. The dual fuel four stroke engine type Wärtsilä L20DF

The object in the publication is a four-stroke dual fuel engine Wärtsilä 6L20DF operating on the lower margin of the high speed range has the characteristics as shown in Table 1.

Table 1: *Engine 6L20DF characteristics*

Wärtsilä 6L20DF	
Cylinder bore	200 mm
Stroke	280 mm
Piston displacement	8.8 l/cyl.
Number of valves	2 inlet valves and 2 exhaust valves
Speed	1200 rpm
Power output	1110 kW

The majority of the existing modern dual fuel engines used in marine applications have the same principle of operation as the above-mentioned engine. These are dual fuel lean burn concept engines [10, 11] which rely on a specific air/fuel ratio to meet the requirements of the IMO tier III NOx emission standard without after treatment of the exhaust gases.

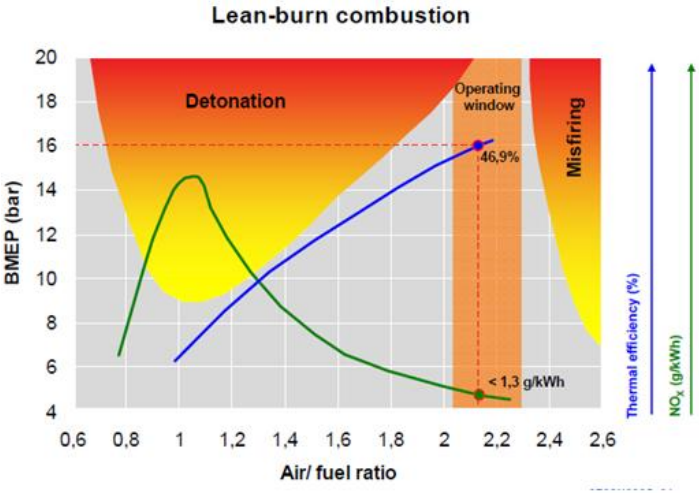


Fig. 1 *Lean burn concept for four stroke dual fuel engines [10].*

With the lean burn engines with fuel-air ratio around 2 it is kept the low NOx emission mode []. On low load ranges the change of the fuel-air ratio outside this limit will lead to increased emissions but as the engine load is increased the deviation in the fuel-air ratio will lead to knocking phenomenon or misfiring. As these are Otto cycle engines, they rely on the mixture compressing in the cylinder and in that case the gas fuel quality would influence the knocking tendency. Steady and controlled combustion and ignition would occur in the case the methane content of the natural gas (corresponding the Methane number) used as fuel is as high as possible. In the available sources of natural gas there is no pure natural gas containing only Methane. There are other hydrocarbon ingredients with usually lower self-ignition temperature than the Methane which generally lowers the resistance of the compressed in the engine cylinder gas on self-ignition. The DF engines manufacturer's set up certain lower limits of the Methane number of the fuels used with the engines, depending on the engine rating at which the engines would be fully operational in the high load range without knocking to occur.

In the cases when the Methane number of the gas fuel is lower the limit set, the sequence of the operation on high loads would be the engine to start knocking. Due to that the manufacturers set derating algorithm for the engine operation with low methane number fuels to protect the engines from harmful uncontrolled combustion. In that case the ship operators should expect what would be the derating extend and what will be the available power of the engines operating on gas to manage proper power management of the ship's electrical plant [3, 7].

The basic comparison between the conventional diesel engine and the dual fuel lean burn engine combustion process shows that with the Diesel cycle engine, due to the non-homogenous fuel-air mixtures even the exceeded amount of air present in the cylinder available, the combustion is stable and there is no necessity to adjust the air-fuel ratio in such extend as with the dual fuel engines. On the flame front there are always rich fuel/air mixtures [11] which keep the combustion fast and steady, although these are the conditions to generate nitrogen oxides and particular matters due to the high peak temperatures. On the other hand, the diesel cycle fuel injection manner has no relation with pre-ignition due to the lack of fuel in the cylinder during the compression stroke. The Diesel cycle operating engines appear that could operate in any condition with sufficient and exceeding amount of air in the cylinder, without tendency to knock or misfire (if no other issues), but the dual fuel engines would require proper fuel-air ratios to be adjusted and controlled during the gas fuel mode, so to keep smooth operation.

3. The experiment

In the present publication it will be reported an experiment with dual fuel engine in gas fuel mode with different grades of natural gas with lower methane number than the required from the engine manufacturer, to present the derating scheme of the engine while reducing the Methane number of the fuel. The experiment is carried out in simulated environment [6, 8, 9, 12] to facilitate the process of use different gas fuel grades as these are the capabilities of the simulator.

They were performed checks on the engine performance on maximum load mode (100% setpoint) of the engine while the Methane number of the gas fuel was gradually reduced from 80 MN to 60 MN as these are the ranges possible to be faced in the real practice with use of LNG as fuel in the IGF code ships, while the bunkered gas fuel weathering process has been developed. The results obtained in the experiment are presented in Table 2.

Table 2: *Engine derating related to the Methane number.*

Methane Number	Engine actual load [%]	Engine set up load [%]
79.94	**99.9**	100
77.49	**97.5**	100
75.03	**95**	100
72.52	**92.5**	100
69.96	**90**	100
67.46	**87.5**	100
64.99	**85**	100
62.47	**82.5**	100
60.03	**80**	100

The data acquired was processed and a linear figure describing the relation between the Methane number and engine derating was established as on Figure 2.

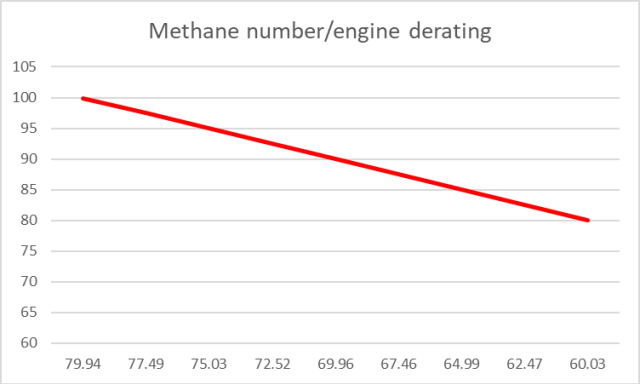


Fig. 2 *Engine derating dependence on the gas fuel methane number*

4. Experiment results analysis

The corresponding derating of the engine on gas mode with natural gas with lower methane number than 80 as it is the lower limit of the manufacturer for normal operation of the entire load range, seems that there would be several specifics which need to be taken in to account while operating the engines in such conditions:

- The bunkered LNG fractions will determine the initial methane number of the fuel in use. In that case the requirement for the quality for the bunker delivery quality must be with as high as possible methane number of the LNG to obtain proper operation of the dual fuel engines.
- The weathering process of the LNG in the tank must be considered and on the base of the initial value to be planned actions to reduce the influence of the dropping methane number by proper power management of the electrical plant.
- In case of deviations between the requested quality and the delivered LNG laboratory analysis to be rejected the receiving of the bunker.
- In case of lower methane number value, as far it is from the lower limit as lower to be the load of the engines so to avoid knocking.
- In case of intended manual adjustment of the load limit of the engines to be considered the specific features of the engine control system and the means of lean burn process control as the ignition timing, fuel air ratio and the charge air system performance.

5. Acknowledgements

The tasks in the publication to be presented experiment and results to be analysed was accomplished. The features of engine derating due to low methane number of the LNG used as fuel shows that there must be additional precautions to be considered by the engineers handling these power plants.

The simulated experiment allows to be carried out different load modes tests of the engines with different grades of fuels, so to facilitate the preparation of the further operation of the engines with the following bunkering batches of LNG.

The outcome of the publication could be beneficial to the marine engineers and superintendents to better understand, clarify and explain the differences in the operation of the dual fuel and the diesel four stroke engines.

6. References

1. D Popov, *Investigation of the influence of diesel fuels (standard diesel fuel and standard diesel fuel after treatment with ANSTOTECH device) on specific fuel oil consumption of marine diesel engine type SKL 3NVD24, XVIII International scientific congress MACHINES. TECHNOLOGIES. MATERIALS*, **YEAR IV, ISSUE 1 (18),** pp 31-34, Borovets, Bulgaria (2021), ISSN 2535-003X (ONLINE).

2. I. Bakalov; D Popov, *Investigation of the influence of diesel fuels (standard diesel fuel and standard diesel fuel after treatment with ANSTOTECH device) on the average temperature of marine diesel engine type SKL 3NVD24, XVIII International scientific congress MACHINES. TECHNOLOGIES. MATERIALS*, **YEAR IV, ISSUE 1 (18)**, pp 34 -38, Borovets, Bulgaria (2021), ISSN 2535-003X (ONLINE).

3. D. Vasilev; H. Hristov; G. Lyutskanov, *Working Parameters of a DP Vessel Power Plant. First International Marine Engineering Conference*, Varna, (2018), pp. 180-186. ISBN 978-619-7428-31-5.

4. H. Hristov; I. Bakalov; B. Shopov; D. Yovkov, *Modeling of the dependence of the produced amount of hydrogen gas (y) on the amperage of cell (x) of a marine diesel engine SKL 3NVD24. Pedagogika-Pedagogy*, **Volume 93**, Number 6s, (2021) (https://doi.org/10.53656/ped21-6s.24mod).

5. H. Hristov; I. Bakalov; B. Shopov; D. Yovkov, *Modeling of the dependence of CO2 contained in the exhaust gases on the amount of hydrogen gas supplied to the engine. Pedagogika-*

Pedagogy, **Volume 93**, **Number 6s**, (2021) (https://doi.org/10.53656/ped21-6s.24mod).

6. H. Hristov; J. Moskov, *Application of mathematical models for evaluating the consequences of damages on crankshaft of slow speed marine diesel engine*, *Морски научен форум*, стр. 69-73, ВВМУ „Н. Й. Вапцаров", (2016), ISSN: 1310-9278.
7. K. Nedev, *An investigation of control system for ship cleaning equipment*, *First International Marine Engineering Conference*, Engineering Faculty Nikola Vaptsarov Naval Academy, Varna, (2018), pp. 141-147. ISBN 978-619-7428-31-5.
8. M. Vasilev, *New challenges against instructors for marine engineers*, *Trans&Motauto* (2015), Varna
9. M. Vasilev, *Usage of FESTO simulator for marine systems*, *Trans&Motauto* (2015), Varna
10. Wartsila land & sea academy, *Wartsila 50DF engine operation manual*, (2010)
11. *Sh. Xu; D. Anderson; M. Hoffman, A phenomenological combustion analysis of a dual-fuel natural-gas diesel engine (2016), Proceedings of the Institution of Mechanical Engineers, Part D: Journal of Automobile Engineering,* **V 231** issue: 1, *pp 66-83, https://doi.org/10.1177/0954407016633337*
12. И. Бакалов, *Използване на симулационен комплекс за провеждане на обучение и тренировки по борба с пожари Морски научен форум*, **том 2**, Варна (2016)
13. И. Бакалов, Р. Бакалова, *Използване на алтернативни горива в корабните дизелови двигатели, икономически фактор*. Шумен, *Конференция с международно участие "MATTEX 2014*". ISSN: 1314-3921 стр. 228 - стр. 232